NANOTECHNOLOGY CHARACTERIZATION LABORATORY

Prepared for C-Sixty Inc., a subsidiary of
Carbon Nanotechnologies, Inc.

Functionalized Fullerenes
NCL200701A
January 2007

Nanotechnology Characterization Laboratory
National Cancer Institute at Frederick
SAIC-Frederick, Inc.
Frederick, MD 21702
(301) 846-6939 • ncl@ncifcrf.gov
http://ncl.cancer.gov

TABLE OF CONTENTS

EXECUTIVE SUMMARY 5

NANOPARTICLE DESCRIPTIONS 7

PHYSICO-CHEMICAL CHARACTERIZATION 9

Section Summary 9
Hydrodynamic Size/Size Distribution via Dynamic Light Scattering (DLS) 10
Ultra Violet–Visible (UV-Vis) Absorbance Spectra 11
Molecular Weight Measurement by Mass Spectrometry (MS) 12
Reversed-Phase HPLC 13
Zeta Potential 16
Capillary Electrophoresis (CE) 17
Capillary Electrophoresis (CE) in Serum Matrix 18

***IN VITRO* TOXICOLOGY 23**

Section Summary 23
LLC-PK1 LDH and MTT Cytotoxicity Assays (GTA-1) 24
LLC-PK1 and HL-60 Trypan Blue Cytotoxicity Assay 29
Cell Cycle Effects of DF1 in HL60 Cells 31
LC-PK1 and Sprague-Dawley Primary Hepatocyte Reactive Oxygen Species Assay (GTA-7) 32

***IN VITRO* CHEMOPROTECTION STUDIES 37**

Section Summary 37
Effect of DF1 Cotreatment on Cisplatin-Induced Apoptosis in LLC-PK1 (GTA-5) 38
Effect of DF1 Pretreatment on Cisplatin-Induced Apoptosis in LLC-PK1 (GTA-5) 40
Effect of DF1-mini Cotreatment on Cisplatin-Induced Apoptosis in LLC-PK1 (GTA-5) 42
Effect of AP12 and AP36 Cotreatment on Cisplatin-Induced Apoptosis in LLC-PK1 (GTA-5) 44
Effect of DF1 Cotreatment on Cisplatin-Induced Lipid Peroxidation (GTA-4) 46

***IN VITRO* IMMUNOLOGICAL CHARACTERIZATION 49**

Section Summary 49
Nanoparticle Hemolytic Properties (ITA-1) 50
Nanoparticle Ability to Induce Platelet Aggregation (ITA-2) 51
Nanoparticle Toxicity to Bone Marrow Cells (ITA-3) 53

CONTRIBUTORS 55

ABBREVIATIONS 57

REFERENCES 59

Executive Summary

The objective of the C-Sixty, Inc. - NCL collaboration is to aid C-Sixty, Inc. in identifying the most promising candidate from a series of fullerene based antioxidants, and to investigate potential applications related to cancer therapy. Water-soluble, functionalized fullerenes have been shown to protect against a broad range of oxidative injuries, including organ reperfusion injury and ionizing radiation. The antioxidant candidates submitted for testing were AF1 (NCL16), AF3 (NCL17), C3 (NCL19), DF1 (NCL42), and DF1-mini (NCL45) (see Figure 1). NCL studies conducted on these candidates can be divided into physico-chemical characterization, *in vitro* toxicology, *in vitro* chemoprotection studies, and *in vitro* immunology. Of the fullerene derivatives, DF1 and DF1-mini were selected for more thorough characterization due to their therapeutic potential.

Physico-Chemical Characterization

Physico-chemical characterization of these samples included Dynamic Light Scattering (DLS) to measure the hydrodynamic size, Reversed Phase High Performance Liquid Chromatography (RP HPLC) and Capillary Electrophoresis (CE) for purity, and Matrix Assisted Laser Desorption/Ionization-Time of Flight Mass Spectrometry (MALDI-TOF MS) for molecular weight and purity. In addition, the zeta potential was also measured for DF1. Unlike the parent compound (C60), which is hydrophobic and insoluble in aqueous buffers, the derivatized fullerenes have a variable degree of aqueous solubility that increases their potential for biological applications. Since there is no currently available method for the detection and quantitation of the fullerene derivatives in matrix, a capillary electrophoresis approach was developed for the analysis of C3 and DF1 in both standard solutions and serum matrix.

Hydrodynamic sizes for these materials, measured by batch-mode DLS, were 4.8 nm for DF1, and 4.0 nm for DF1-mini. Molecular weight analysis by MALDI-TOF Mass spectrometry was in agreement with the proposed structures. Purity as assessed by RP-HPLC and MALDI-TOF MS shows that while both DF1 and DF1-mini contain impurities, the latter (DF1-mini) seems to be relatively purer than its next generation derivative (DF1).

In Vitro Toxicology

The biocompatibility of the functionalized fullerenes was evaluated in porcine renal proximal tubule (LLC-PK1) and human leukemia (HL60) cell lines. AF1 and C3 functionalized fullerenes were found to be minimally cytotoxic, while AF3 and DF1 were nontoxic to LLC-PK1 cells. In HL-60 cells, both DF1 and C3 were found to be cytotoxic. Cell cycle analysis demonstrated that DF1 primarily targeted HL60 cells in the G1 phase. Treatment of renal proximal tubule (LLC-PK1) cells and Sprague-Dawley primary hepatocytes with C3 or AF1 increased levels of reactive oxygen species (ROS), while DF1 decreased ROS levels dose dependently. The observation that DF1 is selective in its cytotoxicity, in that it is toxic to the human leukemia cell line (HL-60), but not the porcine renal proximal tubule cell line, warrants further investigation. Based on this biocompatibility assessment, DF1 was chosen as a promising candidate for therapeutic applications and is therefore the focus of the cisplatin chemoprotection studies which follow. The internalization and subcellular localization of the fluorescent AF3 fullerene derivative in LLC-PK1 cells was examined by

confocal microscopy. Confocal microscopy data suggests that AF3 is internalized and distributes to mitochondria.

In Vitro Chemoprotection Studies

Cisplatin (CP) is an antineoplastic agent used in the treatment of a variety of solid tumors (Go and Adjei, 1999). The most common dose-limiting toxicity encountered during CP therapy is nephrotoxicity, characterized by tubular necrosis and renal failure (Loehrer and Einhorn, 1984). Oxidative stress has been implicated in CP nephrotoxicity, and studies have shown that antioxidants are effective in preventing toxicity in animal models (Atessahin *et al.*, 2005; Francescato *et al.*, 2004; Nishikawa *et al.*, 2001). The present study examined the potential of the dendritic fullerene derivatives, DF1 and DF1-mini, to prevent CP cytotoxicity in porcine proximal tubule cells. The cotreatment of LLC-PK1 cells with DF1 or DF1-mini resulted in partial protection against CP, as determined by cell morphology. Caspase 3 induction, a measure of apoptosis initiation, was also suppressed >50% by either DF1-mini or DF1 cotreatment. Pretreatment with DF1 prior to incubation with CP afforded partial protection against both caspase 3 induction and morphological changes. The fullerene component of DF1 was likely responsible for the observed protection, as the dendritic branches of the derivatized fullerenes independently had no effect The mechanism of the observed DF1 and DF1-mini chemoprotection in LLC-PK1 cells is likely amelioration of CP-induced oxidative stress. Future studies will determine if DF1 or DF1-mini also protects against cisplatin nephrotoxicity *in vivo*, while maintaining cisplatin therapeutic properties.

In Vitro Immunological Characterization

This is a study of the effects of fullerene derivatives on the integrity of red blood cells, platelet aggregation, and formation of granulocyte-macrophage colonies (CFU-GM).. AF1 and AF3 demonstrated hemolytic properties on human erythrocytes, while C3 and DF1 did not affect the integrity of erythrocytes. None of the tested fullerene derivatives induced platelet aggregation, however C3 and DF1 suppressed aggregation of platelets induced by collagen. None of the tested fullerene derivatives were myelosuppressive or capable of preventing cisplatin-induced toxicity to bone marrow haematopoietic stem cells.

Nanoparticle Descriptions

The fullerenes are a family of carbon allotropes named after Richard Buckminster Fuller. A dendrofullerene is a fullerene derivative with an attached branched architecture An amphiphilic fullerene is a fullerene derivative with an attached hydrophilic moiety to render solubility both in aqueous and organic solvents. The fullerene derivative samples (Figure 1) submitted to the NCL by C-Sixty, Inc. are:

NCL16: An amphiphilic fullerene C60 derivative commonly called AF1.
NCL17: An amphiphilic fullerene C60 derivative commonly called AF3.
NCL19: A tris-malonic acid C60 derivative commonly called C3.
NCL42: A dendrofullerene C60 derivative with branched architecture and 18 carboxylic acid terminal groups, commonly called DF1.
NCL45: A dendrofullerene derivative with 6 carboxylic acid terminal groups, referred to here as DF1-mini.

The purpose of this study was to determine a lead antioxidant candidate. Samples which showed the most therapeutic promise received the most extensive characterization.

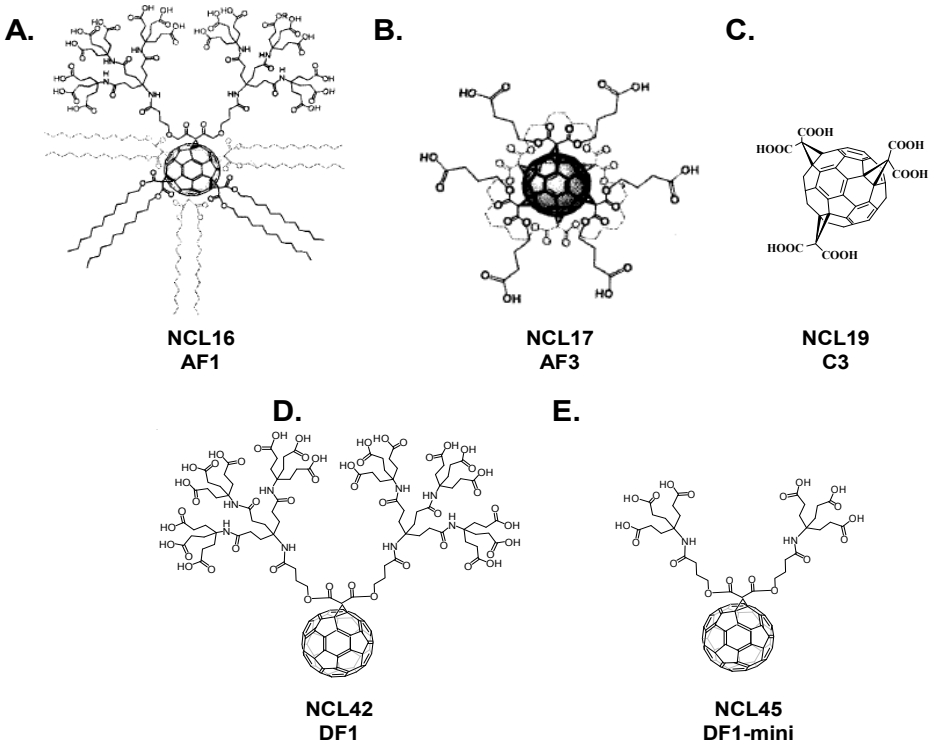

Figure 1. Theoretical molecular structures of the C-Sixty fullerene derivatives and their NCL number designations.

Physico-Chemical Characterization

Section Summary

The main purpose of this collaboration was to identify the most promising candidate from a series of fullerene based antioxidants. Based on preliminary discussions with C-Sixty Inc., it was decided to focus on DF1 and DF1-mini as the leading candidates. Physico-chemical characterization of these two samples included Dynamic Light Scattering (DLS) to measure the hydrodynamic size, Reversed Phase High Performance Liquid Chromatography (RP HPLC) and Capillary Electrophoresis (CE) for purity and Matrix Assisted Laser Desorption/Ionization-Time of Flight Mass Spectrometry (MALDI-TOF MS) for molecular weight and purity. In addition, the zeta potential was also measured for DF1. Unlike the parent compound (C60), which is hydrophobic and insoluble in aqueous buffers, the derivatized fullerenes have variable degree of aqueous solubility that increases their potential for biological applications. Since there is no current available method for the detection and quantitation of the fullerene derivatives in matrix, a capillary electrophoresis approach for the analysis of C3 and DF1 in both standard solutions and a serum matrix was developed. The quantitation of the particles was linear from 0-500 µg/mL with quantitation limits ranging from 0.6 to 6 µg/mL.

Hydrodynamic sizes for these materials, measured by batch-mode DLS, were 4.8 nm for DF1, and 4.0 nm for DF1-mini. Molecular weight analysis by MALDI-TOF Mass spectrometry was in agreement with the proposed structures. Purity as assessed by RP-HPLC and MALDI-TOF MS shows that while both DF1 and DF1-mini contain impurities, the latter (DF1-mini) seems to be relatively purer than its next generation derivative (DF1).

Hydrodynamic Size/Size Distribution via Dynamic Light Scattering (DLS)

Design and Methods

Hydrodynamic size (diameter) of DF1 and DF1-mini were measured in 10 mM NaCl using DLS at 25° C. An instrument with back scattering detector was used for these measurements in batch mode (no fractionation). Samples were weighed and dissolved in 10 mM NaCl to give a final concentration of 1 mg/mL. Samples were filtered through a 0.02µ filter before taking a minimum of nine measurements.

Results

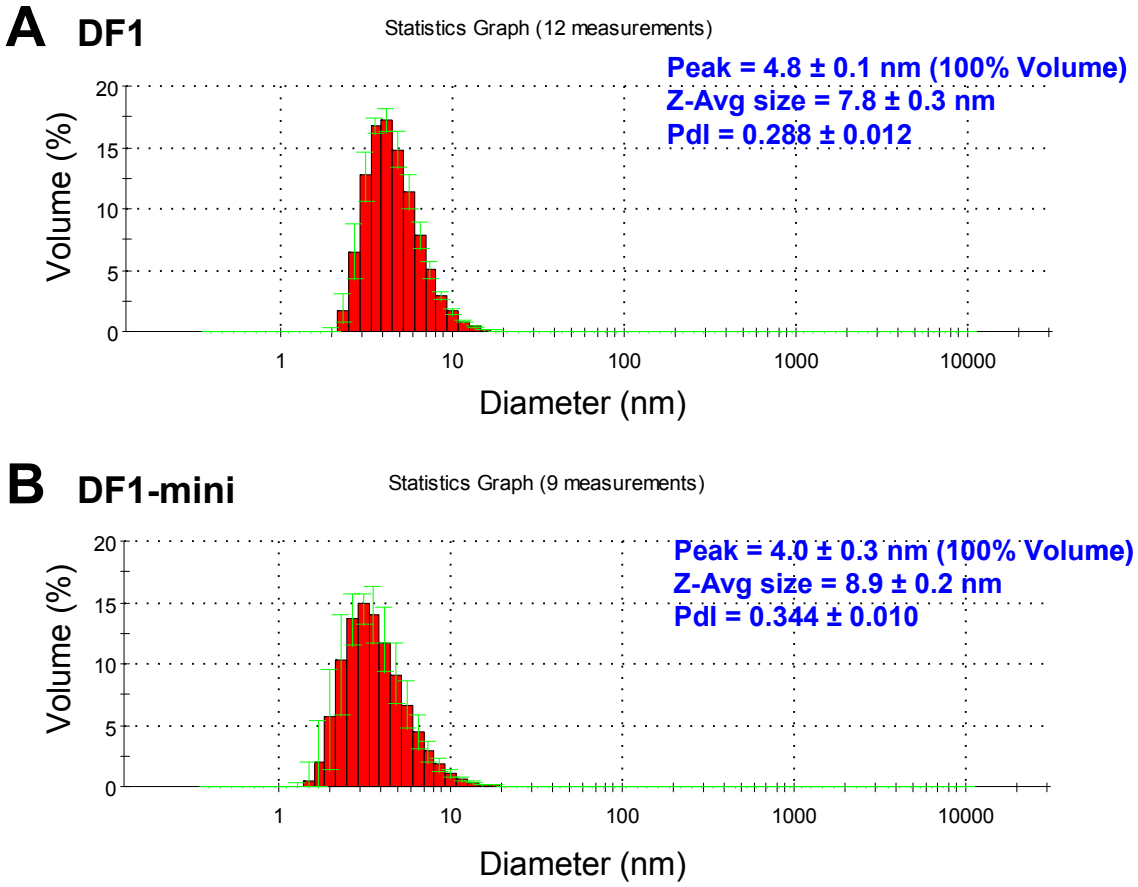

Figure 2. Volume distribution plot for (A) DF1 and (B) DF1-mini in 10 mM NaCl.

Analysis and Conclusions

The Z-avg size, which is more sensitive to larger size species in the sample, of DF1 is 7.8 nm. The Z-avg size of DF1-mini is 8.9 nm. There is only a slight difference in the volume-weighted size (denoted as 'Peak' in Figure 2) between the two conjugates, with DF1 being slightly larger (4.8 nm) than DF1-mini (4.0 nm) as expected. This data also suggests that under these buffer conditions, there is little or no aggregation in these samples.

Ultra Violet–Visible (UV-Vis) Absorbance Spectra

Design and Methods

UV-Vis spectra were recorded using a Thermo Electron Evolution 300 spectrophotometer (Waltham, MA). Samples were prepared in HPLC-grade water and measured in quartz microcuvettes (with light path length, b = 10 mm, QS109.004, Hellma, Plainview, NY).

Results

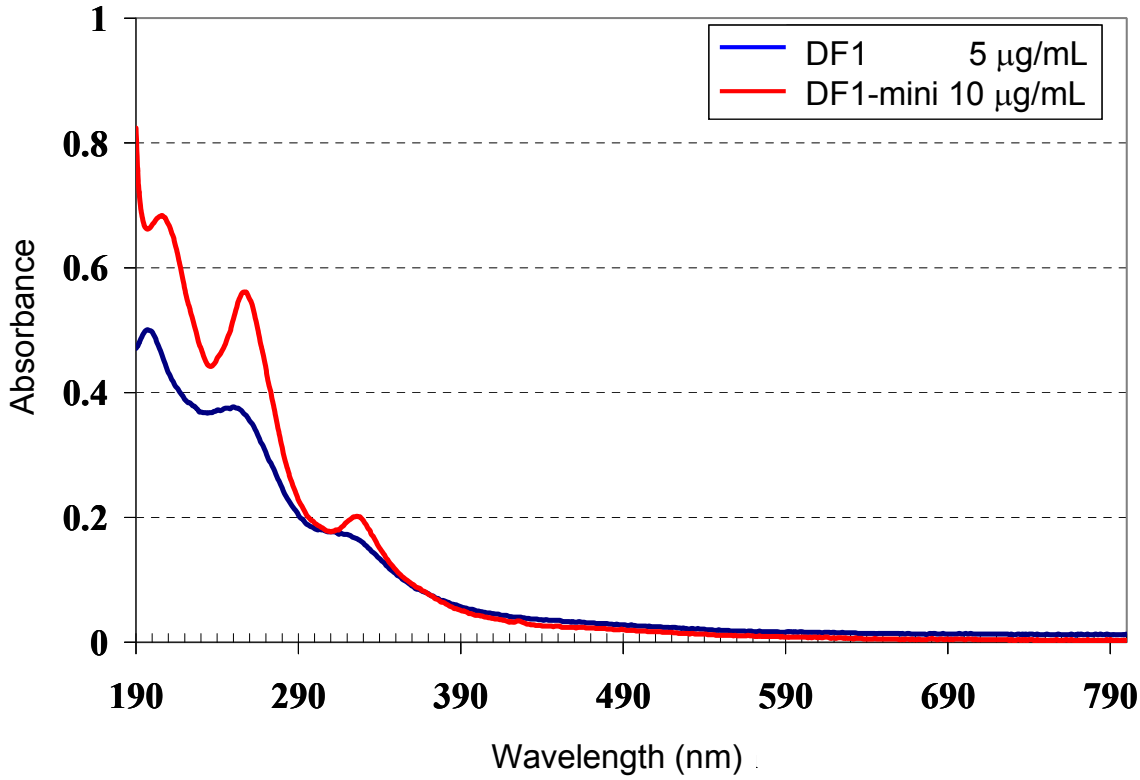

Figure 3. UV-Vis spectra for DF1 and DF1-mini.

Analysis and Conclusions

DF1 and DF1-mini have similar UV-Vis absorption spectra as expected. The peaks at 256 nm and 325 nm are at characteristic wavelengths for absorbance of the fullerene ring and are at approximately the same wavelengths (as expected) for DF1 and DF1-mini. The peaks around 200 nm are attributed to absorbance in the dendrimer branches. There is a small shift in the λ_{max} of this peak between the spectra of the DF1 and DF1-mini samples. The λ_{max} of the lowest wavelength peak in the DF1 spectrum is at a lower wavelength than that of the analogous peak in the DF1-mini spectrum.

Molecular Weight Measurement by Mass Spectrometry (MS)

Design and Methods

Mass spectra were obtained for DF1 and DF1-Mini using matrix assisted laser desorption/ionization-time of flight mass spectrometry (MALDI-TOF MS) in DHB matrix, at 10mg/mL and CH_3CN/H_2O =3/7 (v/v) in positive-ion mode.

Results

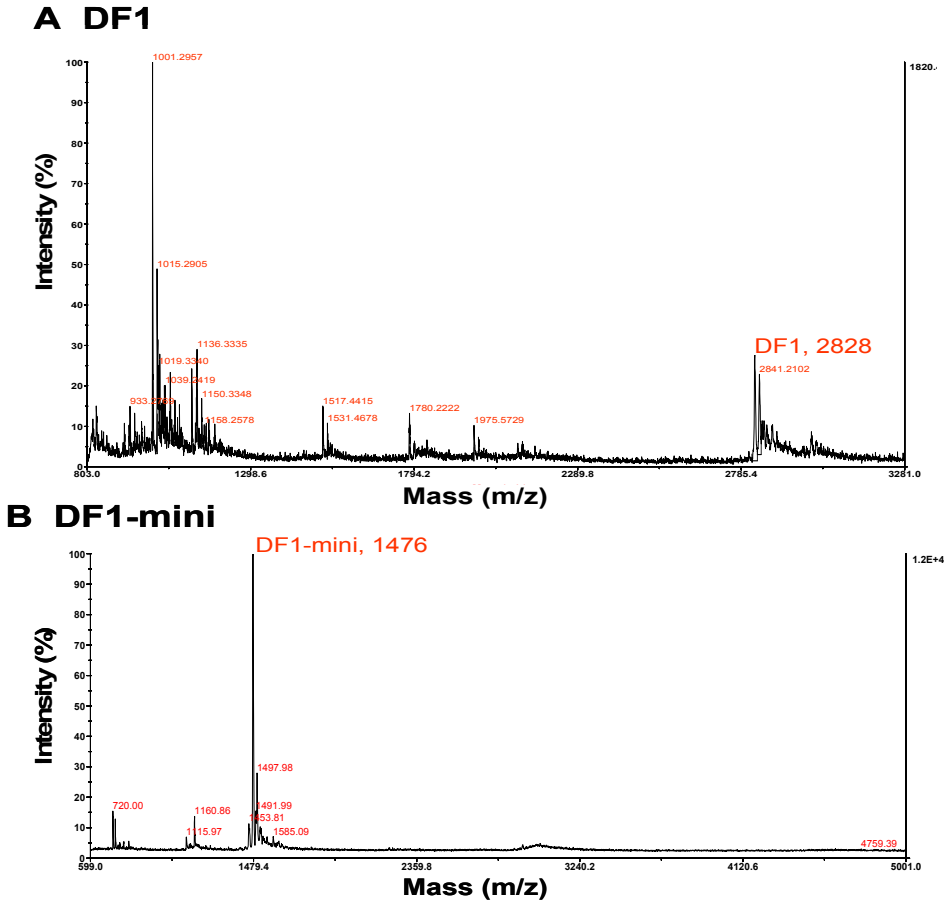

Figure 4. Mass spectra for (A) DF1 and (B) DF1-mini.

Analysis and Conclusions

The theoretical molecular weights of DF1 and DF1-mini are 2828 Da and 1452 Da, respectively. The experimental molecular weight determined from the mass spectra were 2827 Da for DF1 and 1476 Da (which corresponds to 1452 Da plus the mass of a sodium ion) for DF1-mini. The spectrum of the DF1 sample (A) contains several peaks in addition to the peak corresponding to DF1, suggesting the sample contains impurities or fragments due to MS conditions. Minor peaks (e.g., the peak at 720 Da which corresponds to a fullerene ring without any dendritic branches) are also present in the spectrum of DF1-mini (B) and suggest that minor impurities are also present in this sample.

Reversed-Phase HPLC

Design and Methods

Reversed-phase high performance liquid chromatography (RP-HPLC) is a separation technique used for determining the purity of a sample. It is based on the partitioning of the sample molecules with the mobile phase and the stationary hydrophobic phase. The chromatographic system used here consisted of a degasser (Agilent G1379A, Palo Alto, CA), capillary pump (Agilent G1378A), micro well-plate autosampler (Agilent G1377A), Zorbax 300SB-C18 column (1.0 mm ID x 150 mm, 3.5 μm, Agilent), and a diode array detector (Agilent G1315B). The mobile phase consisted of water/acetonitrile (HPLC Grade, 0.14 % (w/v) trifluoroacetic acid) at varying volume percentages with a flow rate of 50 μL/min. The elution profile is illustrated in red and the chromatogram is shown in blue in Figure 5. The injected sample had a concentration of 1mg/mL in a volume of 5 μL (in HPLC water). The eluted sample was detected at 254 nm. Samples were run in triplicate.

Results

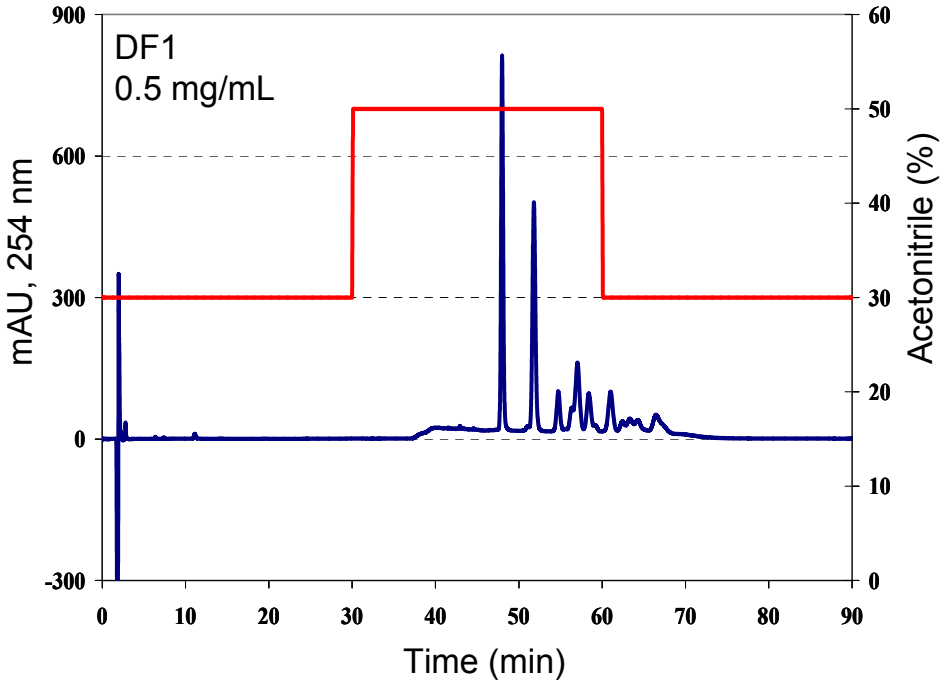

Figure 5. RP-HPLC chromatogram for DF1. See Table 1 for peak retention times and percent areas.

Peak #	Retention Time (min)	% Area	Std Dev (N=3)
1	**48.0**	**29.7**	**0.4**
2	51.1	0.7	0.2
3	**51.8**	**26.3**	**0.1**
4	54.7	4.8	0.1
5	56.4	2.7	0.2
6	**57.0**	**10.4**	**0.1**
7	58.4	5.8	0.3
8	59.2	0.8	0.2
9	61.0	6.8	0.3
10	62.5	1.7	0.1
11	63.3	2.7	0.2
12	64.3	2.4	0.1
13	66.5	5.2	0.3

Table 1. The retention times, percentage of the area and standard deviation (N = 3), for DF1 as determined by RP-HPLC (Figure 5).

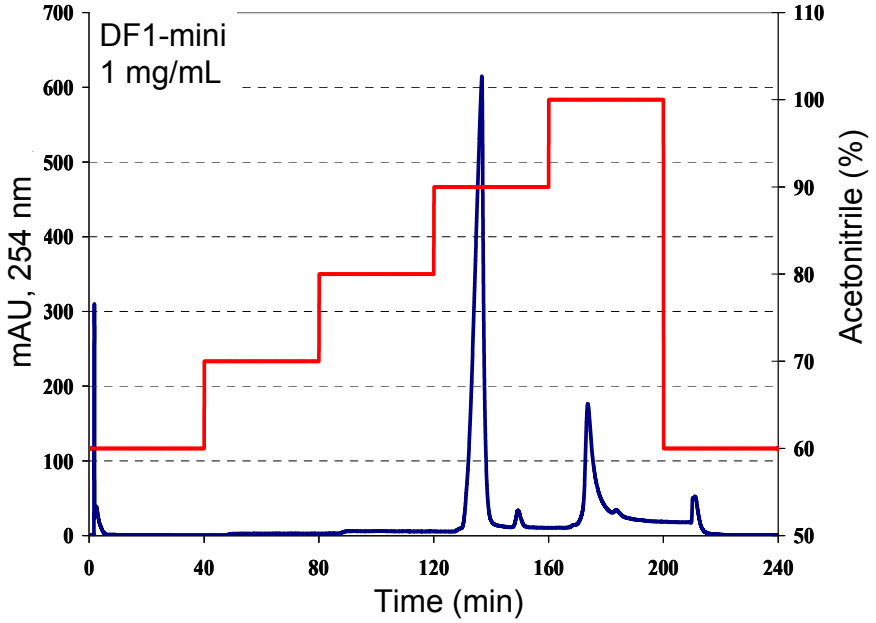

Figure 6. The RP-HPLC chromatogram and elution profile for DF1-mini. See Table 2 for peak retention times and percent areas.

Peak #	Retention Time (min)	% Area	Std Dev (N=3)
1	**136.8**	**75.7**	**6.8**
2	149.3	1.5	0.2
3	**173.7**	**19.3**	**6.3**
4	183.7	0.4	0.1
5	**210.6**	**3.0**	**0.5**

Table 2. The retention times, percentage of the area and standard deviation (N = 3), for DF1-mini as determined by RP-HPLC (Figure 6).

Analysis and Conclusions

For DF1, the UV spectra (data not shown) for the peaks (see Figure 5) highlighted in cyan in Table 1 are consistent with that of DF1 measured with a UV-Vis spectrophotometer. The UV spectral analysis on the remaining peaks showed similar absorption peaks but were slightly shifted to lower wavelengths (blue-shifted by ~10 nm). The UV absorption at these wavelengths is indicative of the presence of fullerene and not free dendritic branches. This data is consistent with published reports by Gharbi et al. (*Anal. Chem*. **2003**, 75, 4217-4222).

For DF1-Mini, the UV spectra (data not shown) for the peaks (see Figure 6) highlighted in cyan in Table 2 are consistent with that of DF1-mini measured with a UV-Vis spectrophotometer. The UV spectral analysis on the remaining two peaks showed a major peak at 225 nm and a minor peak at 254 nm suggesting that these impurities contain the fullerene component. DF1-mini seems to be relatively purer than the next generation derivative (DF1). This is also consistent with mass spectrometry analysis on these two derivatives. Further analysis with LC-MS would provide additional details on the species present as impurities in these two samples.

Zeta Potential

Design and Methods

Samples were diluted in 10 mM NaCl to give a 2 mg/mL final concentration (pH 5.4). A folded capillary cell was used to make these measurements. A minimum of ten measurements were taken for each sample at 25 °C. The applied voltage was 90 V.

Results

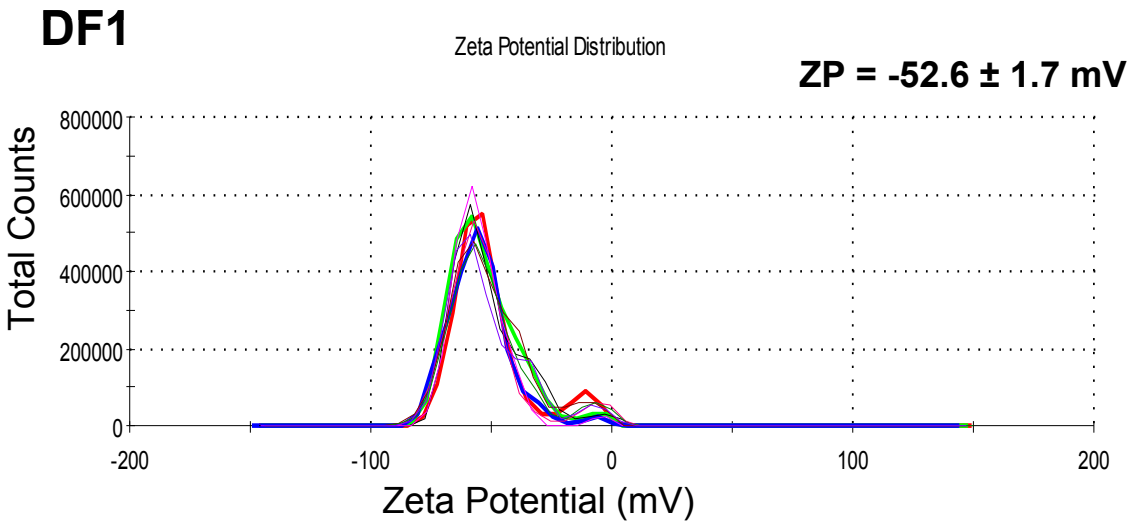

Figure 7. The zeta potential distribution derived from the electrophoretic mobility for DF1 in 10 mM NaCl.

Analysis and Conclusions

The measured zeta potential (-53.6 mV) is negative as expected for a fullerene ring with carboxylated dendritic branches.

Capillary Electrophoresis (CE)

Design and Methods

Capillary Electrophoresis (CE) is a powerful chromatographic technique that separates analytes on the basis of electrophoretic mobility differences. Mobility is determined by the mass to charge ratio of the analyte. CE has high separation efficiencies, high sensitivity, short run times and high automation capability. Sample concentration 0.1 mg/mL in water, capillary Sample preparation: all stock samples were prepared in 50% acetonitrile as 1mg/mL solutions and stored at -40 °C. The stock solutions were diluted 10-fold with water before capillary electrophoresis (0.1mg/mL final concentration). Running conditions: capillary: 60cm ×50 μm I.D; buffer: 10mM sodium tetraborate; separation voltage: 22kV; injection pressure: 20s/0.5 psi/20s; detector: UV (wavelength 200nm). The capillary was rinsed sequentially with 1N sodium hydroxide, water, and the CE buffer between runs.

Results

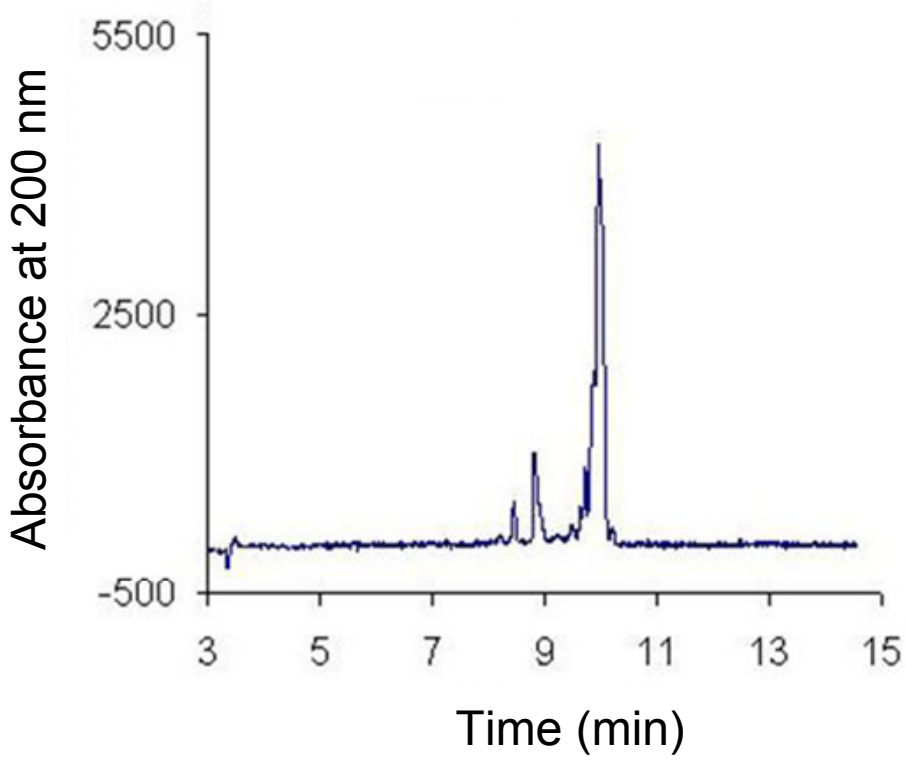

Figure 8. Electropherogram of DF1.

Analysis and Conclusions

The chromatogram shows a major peak eluting at ~10 minutes with several minor peaks eluting before. This suggests that DF1 contains impurities and is consistent with the RP-HPLC data.

Capillary Electrophoresis (CE) in Serum Matrix

Design and Methods

To facilitate *in vivo* studies for the detection and quantitation of the fullerene derivatives in matrix, a CE method was developed for serum incubated samples. Capillary electrophoresis was performed using a Beckman MDQ system (Fullerton, CA, USA) equipped with a photo-diode-array detector. All electropherograms were plotted using the 260 nm channel data. Separations were carried out at room temperature using 50 µm inner diameter fused-silica capillaries with lengths of 40 or 60 cm (L_d=30 or 50 cm). Samples were injected by applying pressure (0.5 psi) for 20 seconds. The field strength for separation was approximately 350 V/cm. Stock solutions of DF1 and C3 were prepared at a final concentration of 1 mg/mL in 50% acetonitrile/H_2O and stored at -40 $^{\circ}$C until used. Prior to CE analysis, aliquots of the stock solutions were lyophilized and reconstituted in PBS or human serum. Nanoparticle samples prepared in human serum were incubated at room temperature for at least 3 hours before use. All serum samples were diluted five-fold with H_2O or SDS solutions of various concentrations before CE analysis. For Capillary Zone Electrophoresis (CZE) and Micellar Electro Kinetic Chromatography (MEKC), a capillary was sequentially washed for one minute with 1 N NaOH, H_2O, and separation buffers between sample injections. A dynamic coating procedure was used for CZE experiments with suppressed electro-osmotic flow.

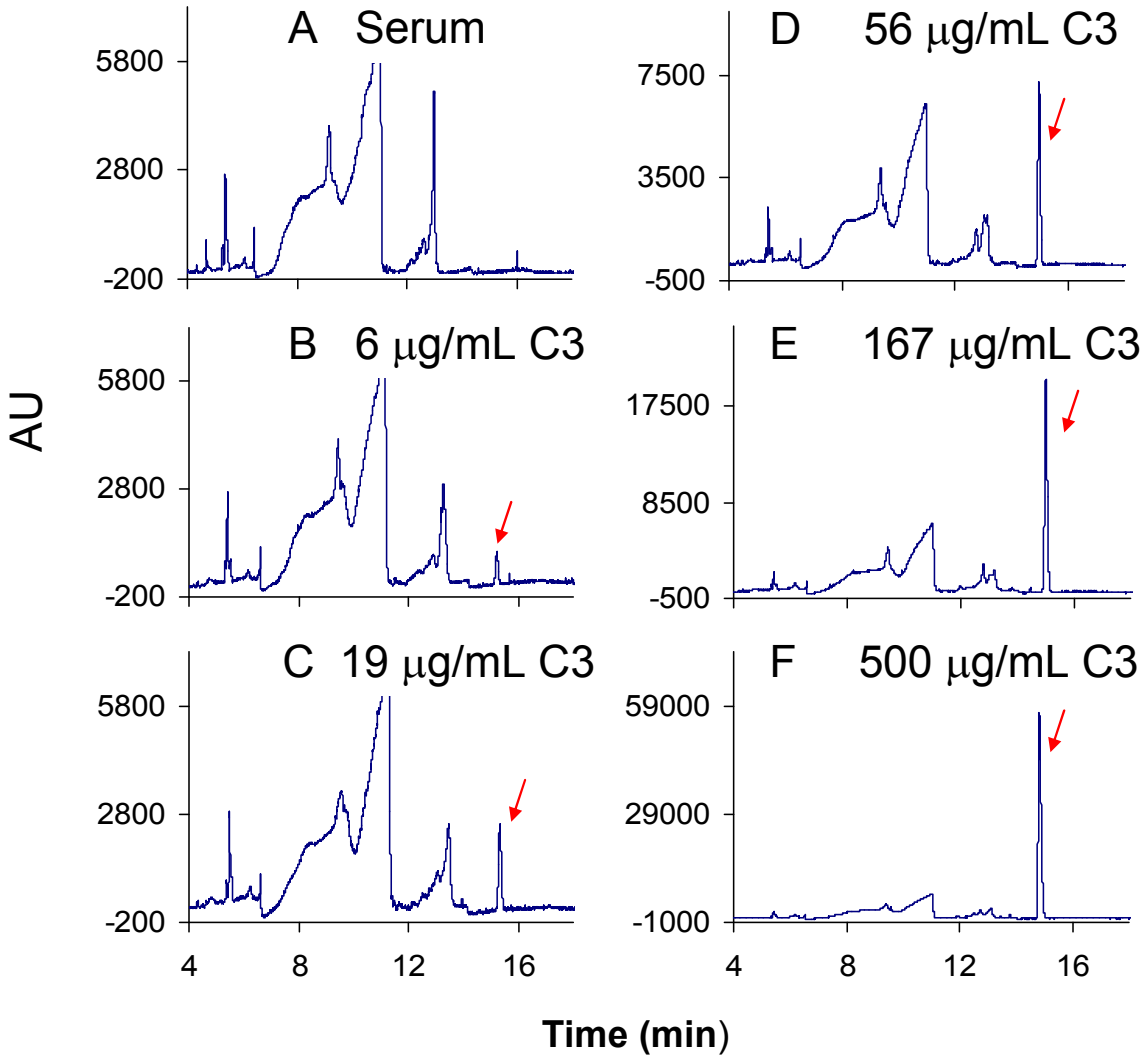

Figure 9. Calibration of carboxyfullerene (C3) in serum using micellar electrokinetic chromatography. Capillary: 50 µm x 40 cm; buffer: 10 mM sodium tetraborate (pH 9.2) with 150 mM SDS; voltage: +14 kV. Serum samples were diluted 5-fold with water and the C3 concentrations refer to the undiluted samples.

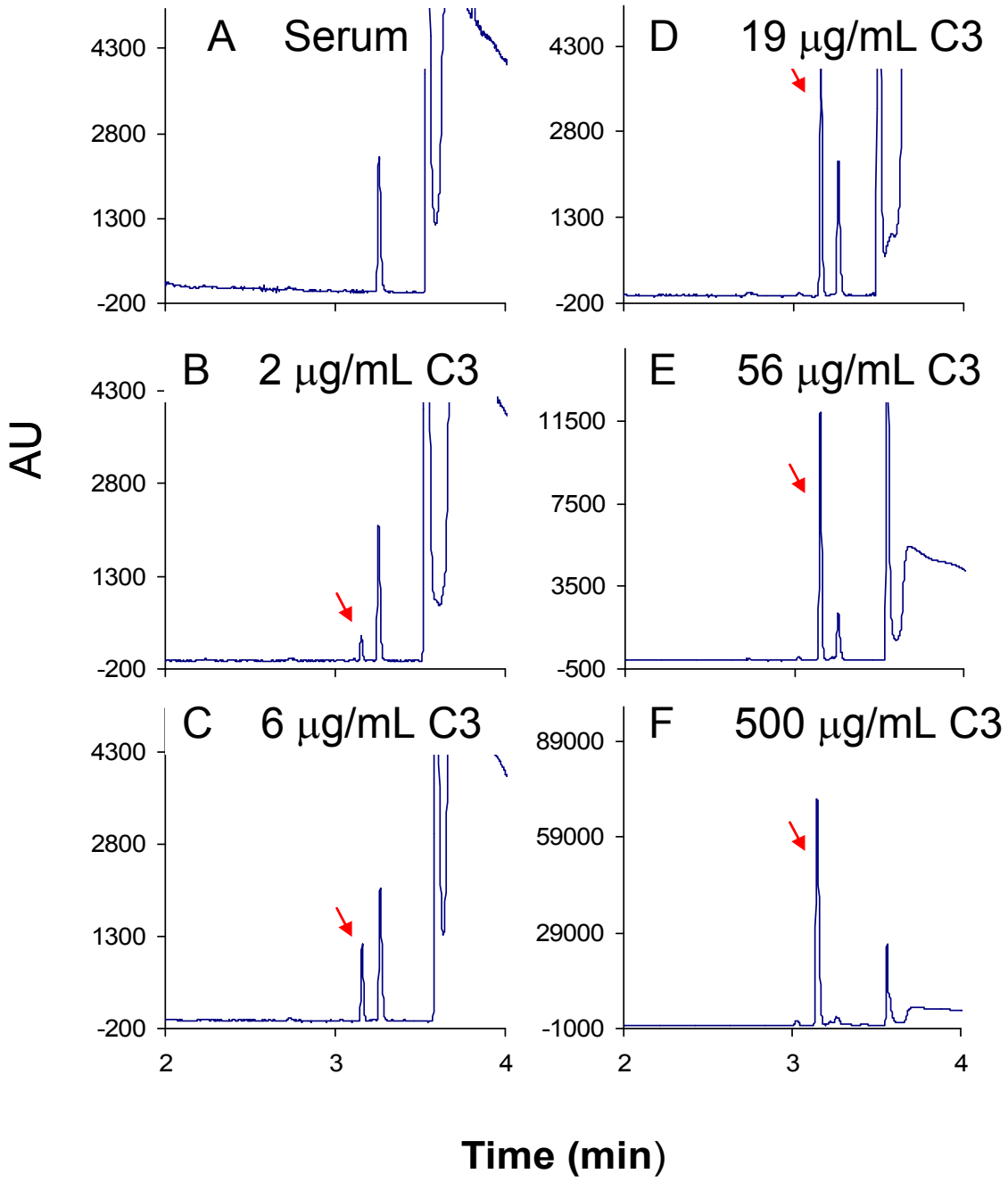

Figure 10. Calibration of carboxyfullerene (C3) in serum using capillary zone electrophoresis. Capillary: 50 µm x 40 cm with dynamic coating; buffer: 40 mM sodium phosphate (pH 7.4); voltage: -14 kV. Serum samples were diluted 5-fold with SDS solution (80 mM final concentration). The C3 concentrations refer to the undiluted samples.

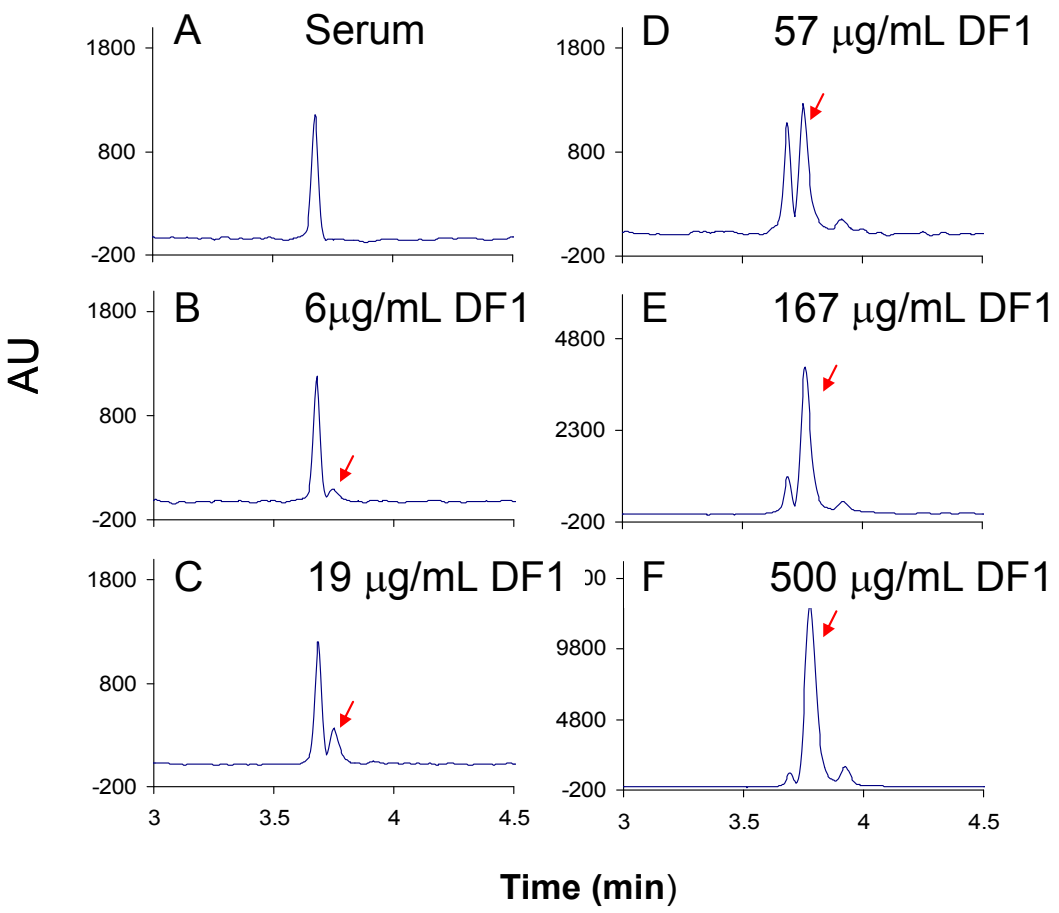

Figure 11. Calibration of dendrofullerence (DF1) in serum using capillary zone electrophoresis. Capillary: 50 µm x 40 cm with dynamic coating; buffer: 40 mM sodium tetraborate (pH 9.2); voltage: -14 kV. Serum samples were diluted 5-fold with SDS solution (20 mM final concentration). The DF1 concentrations refer to the undiluted samples.

Analysis and Conclusions

The calibration curve of C3 in serum using the optimized condition is shown in Figure 9. The peak area versus the C3 concentration is linear from 0-500 µg/mL (R^2 = 0.9998) with a quantitation limit (S/N=3) of approximately 2 µg/mL. The recovery of the assay, calculated by comparing the peak area of100 µg/mL C3 spiked in human serum to that in PBS, is approximately 108%.

The CZE calibration of C3 in human serum treated with 80 mM SDS is shown in Figure 10. The peak area versus the concentration plot is linear from 0-500 µg/mL (R^2 = 0.999) with a quantitation limit (S/N =3) of approximately 0.6 µg/mL. The recovery of the assay, calculated by comparing the peak area of 0.1 mg/ml C3 spiked in human serum to that in PBS, is approximately 104%.

The DF1 calibration in serum with the borate buffer after addition of 20 mM SDS prior to CZE analysis is shown in Figure 11. The peak area versus the concentration plot is linear from 0 to 500 µg/ml (R^2 =0.997), with a quantitation limit of detection approximately 6 µg/mL

(S/N=3). By comparing the peak area of DF1 in PBS to that in serum, the recovery of the DF1 using CZE with the 20 mM SDS treatment protocol is approximately 60.

This CE method can be utilized both for quality control purposes, to test batch-to-batch variability, and for the detection and quantitation of the two fullerene derivatives studied in matrix. This method can be further utilized for other similar nanomaterial samples with minor modifications.

In Vitro Toxicology

Section Summary

The biocompatibility of the functionalized fullerenes was evaluated in porcine renal proximal tubule (LLC-PK1) and human leukemia (HL60) cell lines. AF1 and C3 functionalized fullerenes were found to be minimally cytotoxic, while AF3 and DF1 were nontoxic to LLC-PK1 cells, as determined by the MTT, LDH and trypan blue dye-exclusion assays (Figures 12 - 15, Table 3). The 48 hour IC_{50} values for AF1 and C3 in LLC-PK1 cells were 0.216 (0.044-0.388, 95% CI) mg/mL and 0.143 (0.100 – 0.187, 95% CI) mg/mL, respectively (Figure 14, Table 3). In HL-60 cells, both DF1 and C3 were found to be cytotoxic, as determined by the trypan blue dye-exclusion assay, at the 0.25 mg/mL concentration tested (Figure 15). Cell cycle analysis demonstrated that DF1 primarily targeted HL60 cells in the G1 phase (Figure 16). Treatment of renal proximal tubule (LLC-PK1) cells and Sprague-Dawley primary hepatocytes with 0.004-1.0 mg/mL of C3 or AF1 increased levels of reactive oxygen species (ROS) in a linear fashion, while DF1 decreased ROS levels dose dependently (Figures 17 and 18). Since functionalized fullerenes have previously been shown to have the potential to induce oxidative stress (Sayes et al., 2004), and AF1 and C3 were found to increase ROS generation, it is likely that oxidative stress plays a role in the mechanism of AF1 and C3 cytotoxicity. The observation that DF1 is selective in its cytotoxicity, in that it is toxic to the human leukemia cell line (HL-60), but not the porcine renal proximal tubule cell line, warrants further investigation. Based on this biocompatibility assessment, DF1 was chosen as a promising candidate for therapeutic applications and is therefore the focus of the cisplatin chemoprotection studies which follow. The internalization and subcellular localization of the fluorescent AF3 fullerene derivative in LLC-PK1 cells was examined by confocal microscopy. Confocal microscopy data suggests that AF3 is internalized and distributes to mitochondria.

LLC-PK1 LDH and MTT Cytotoxicity Assays (GTA-1)

Design and Methods

The objective of this study was to determine if AF1, AF3, DF1, or C3 were cytotoxic to porcine renal proximal tubule (LLC-PK1) cells.

Cytotoxicity was determined as described in the NCL method, LLC-PK1 Kidney Cytotoxicity Assay (GTA-1)**.** Briefly, test materials were solubilized via sonication and diluted to the desired assay concentrations in cell culture media (0.004-1 mg/mL). Cells were plated in a 96-well, microtiter plate format. Cells were preincubated for 24 hours prior to test material addition, reaching an approximate confluence of 80%. Cells were then exposed to test material for 6, 24, and 48 hours in the dark, and cytotoxicity was determined using the MTT cell viability and LDH membrane integrity assays. In order to estimate IC_{50} values, the MTT cytotoxicity assay dose-response curves were fit to a sigmoidal Hill equation, $E = Emax\ C^{\gamma}/(C^{\gamma} + IC_{50}^{\gamma})$, using nonlinear regression analysis (Figure 14) (WinNonlin, Pharsight Corp., Mountain View, CA).

Results

The maximum concentration of AF1, AF3, DF1 and C3 tested in the LLC-PK1 cytotoxicity study was 1.0 mg/mL. Neither AF3 nor DF1 produced any measurable loss of cell viability, as determined by the MTT assay, or loss of membrane integrity, as determined by LDH assay at the concentrations tested (Data not shown). Treatment of cells with AF1 or C3, however, resulted in a dose-responsive loss of cell viability (Figures 12 and 13), as measured by MTT assay, and a minor, non-dose responsive loss of membrane integrity (Figure 12 and 13), as measured by LDH leakage. The IC_{50} values, estimated from the nonlinear regression analysis of the MTT assay dose-response curves, were 0.143 (0.100 – 0.187, 95% CI) mg/mL and 0.216 (0.044-0.388, 95% CI) mg/mL, for AF1 and C3, respectively (Figure 14, Table 3).

AF1, AF3 and DF1 were determined to be nontoxic, while C3 was determined to be minimally toxic, to LLC-PK1 cells under these assay conditions. DF1 and C3 were found to be minimally toxic to HL60 cells under these assay conditions.

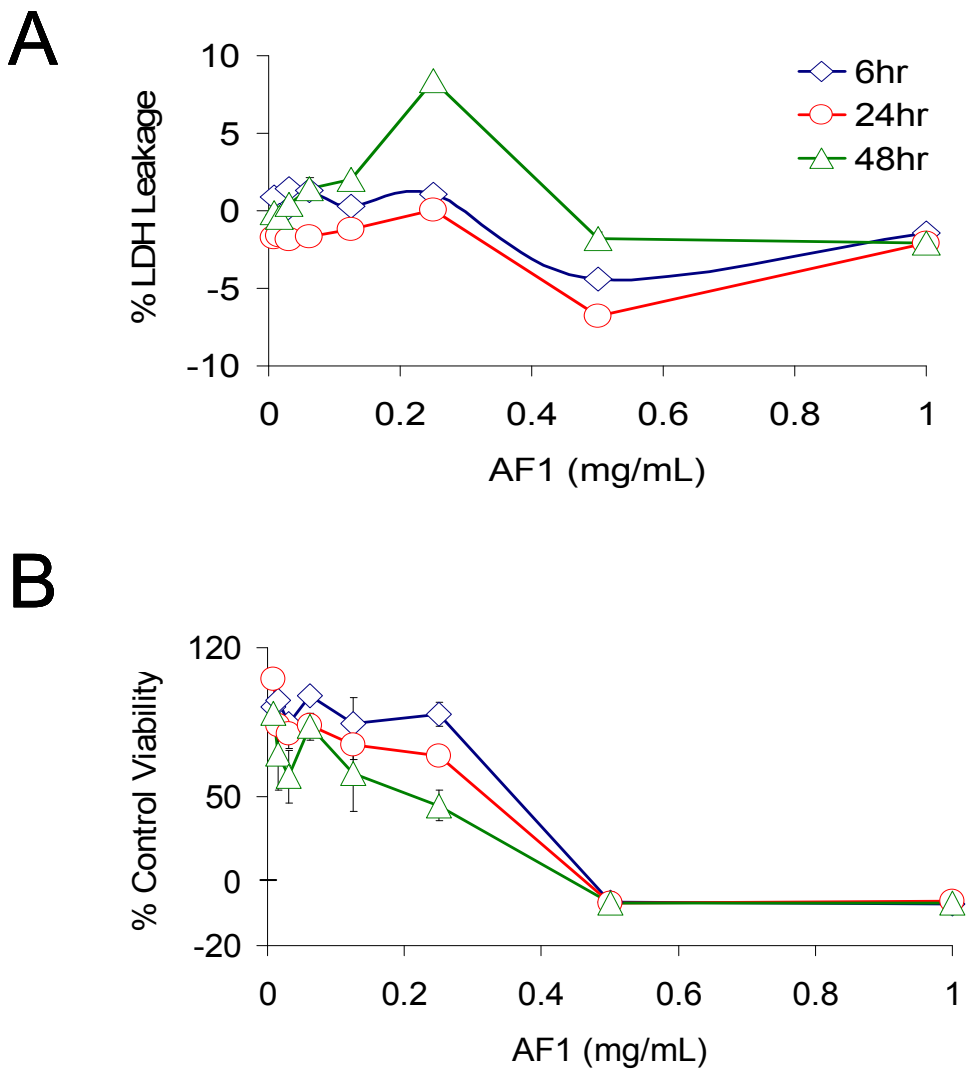

Figure 12. Cytotoxicity of AF1 assayed in LLC-PK1 cells. Porcine renal proximal tubule cells were treated for 6, 24, and 48 hours with 0.004-1.0 mg/mL of test sample. Cytotoxicity at each time point was determined by the LDH (A) and MTT (B) assays, as described in the LLC-PK1 Kidney Cytotoxicity Assay (GTA-1). The data points are the mean ± the standard error, with *N*=3.

A

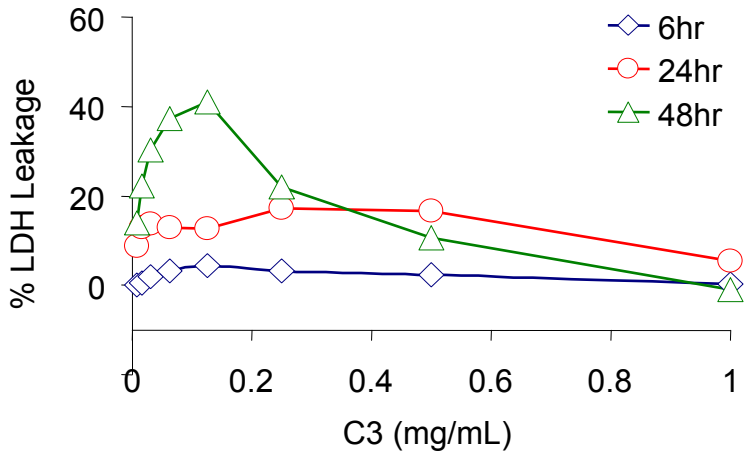

B

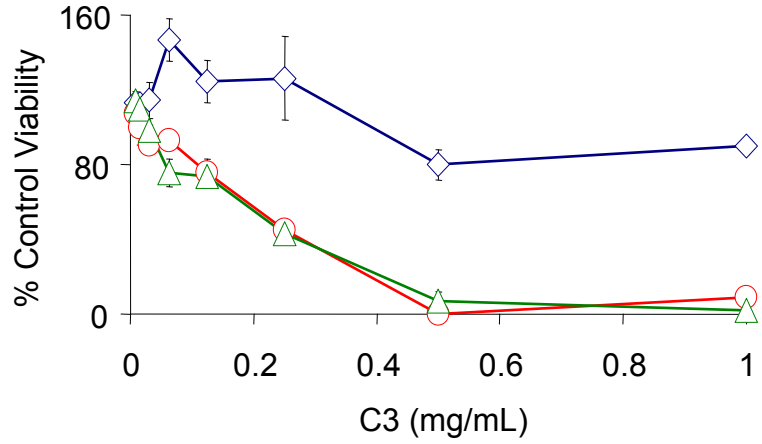

Figure 13. C3 cytotoxicity assayed in LLC-PK1 cells. Porcine renal proximal tubule cells were treated for 6, 24, and 48 hours with 0.004-1.0 mg/mL of test sample. Cytotoxicity at each time point was determined by the LDH (A) and MTT (B) assays, as described in the LLC-PK1 Kidney Cytotoxicity Assay (GTA-1)**.** The data points are the mean ± the standard error, with *N*=3.

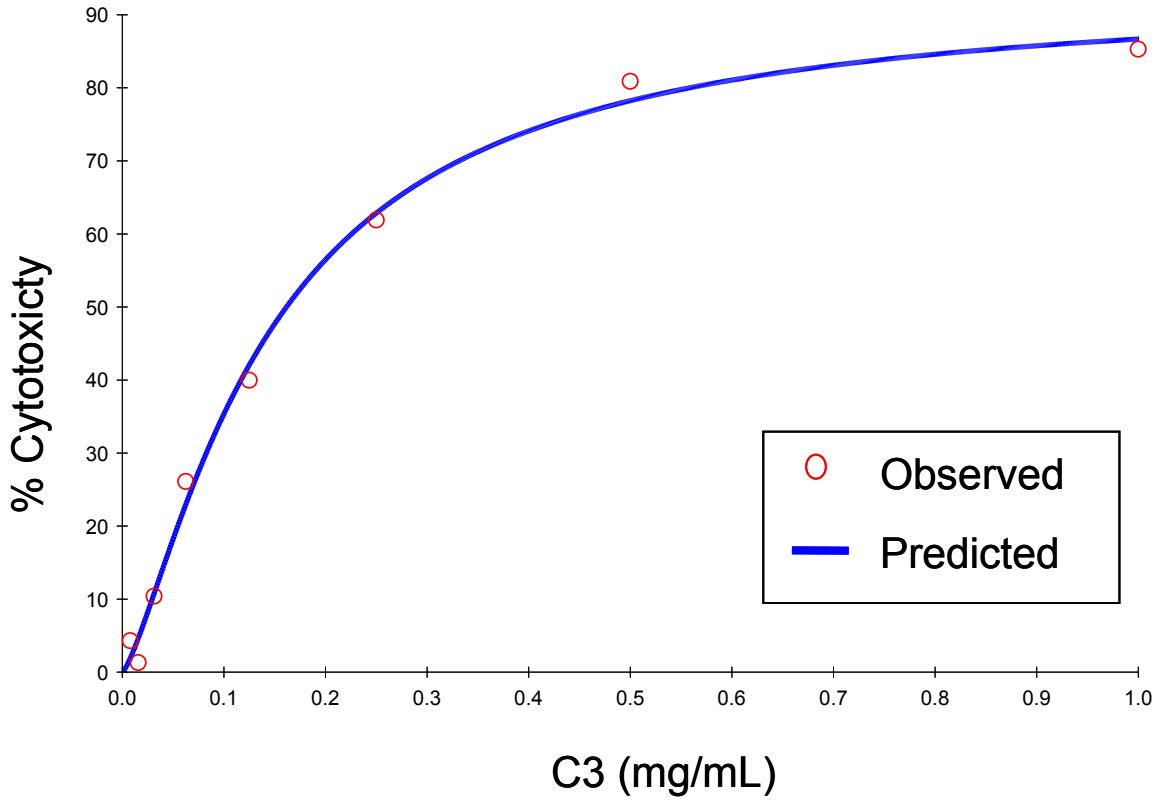

Figure 14. Nonlinear Regression of the Dependence of Percent Cytotoxicty on C3 Concentration. This graph displays the nonlinear fit of the 48 hour C3 MTT data to a sigmoidal Hill equation using the WinNonlin analysis software. The percent cytotoxicity versus the C3 concentration is displayed. The IC_{50} value determined from the fit is 0.145 (0.100 – 0.187, 95% CI) mg/mL.

Sample	IC_{50} (mg/mL)
C3	0.143(0.100-0.187)
DF1	Nontoxic
AF1	0.216 (0.44-0.388)
AF3	Nontoxic

Table 3. MTT cytotoxicity assay in LLC-PK1 cells. LLC-PK1 cells were treated for 48 hours, with 0.004-1.0 mg/mL of test sample. Cytotoxicity was determined by the MTT assay, as described in LLC-PK1 Kidney Cytotoxicity Assay (GTA-1). IC_{50} values were determined by nonlinear regression analysis of the 48 hour MTT cytotoxicity dose-response curves. Data is presented as IC_{50} (95% CI).

Analysis and Conclusions

AF3 and DF1 were determined to be nontoxic in the LLC-PK1 cells, under these assay conditions. AF1 and C3 were determined to be minimally toxic by both MTT and LDH assay.

LLC-PK1 and HL-60 Trypan Blue Cytotoxicity Assay

Design and Methods

The objective of this study was to determine if AF1, AF3, DF1, or C3 were cytotoxic to porcine renal proximal tubule (LLC-PK1) or human leukemia (HL-60) cell lines.

Cytotoxicity was determined by the trypan blue dye exclusion assay**.** Test materials were solubilized via sonication and diluted to the 0.25 mg/mL test concentration. LLC-PK1 and HL60 cells were plated in 35mm, 6-well plates. Cells were preincubated for 24 hours prior to test material addition, reaching an approximate confluence of 80%. Cells were then exposed to the test material for 24 hours in the dark, and cytotoxicity was determined using the trypan blue dye exclusion cell viability assay. Briefly, trypsinized LLC-PK1 and HL60 cells were diluted 1:10 with 0.08% trypan blue in PBS, stained for 5 minutes, and counted with a hemocytometer. Cell viability was determined by counting the number of live cells, which exclude the dye, versus the number of dead cells, which are stained.

Results

The test concentration of AF1, AF3, DF1 and C3 utilized in the LLC-PK1 and HL60 cell trypan blue cytotoxicity assays was 0.25 mg/mL. Treatment of LLC-PK1 cells with AF1, AF3 or DF1 for 24 hours, did not produce a significant loss of cell viability, as determined by the trypan blue dye-exclusion assay (Figure 15A). However, treatment of LLC-PK1 cells with C3, at the same test concentration and exposure period, resulted in a significant loss of cell viability compared to media treated control (Figure 15A). Treatment of HL60 cells with either DF1 or C3, resulted in a significant loss of cell viability (Figure 15B), as measured by the trypan blue exclusion assay.

Analysis and Conclusions

AF1, AF3 and DF1 were determined to be nontoxic, while C3 was determined to be minimally toxic, to LLC-PK1 cells under these assay conditions. DF1 and C3 were found to be minimally toxic to HL60 cells under these assay conditions.

A

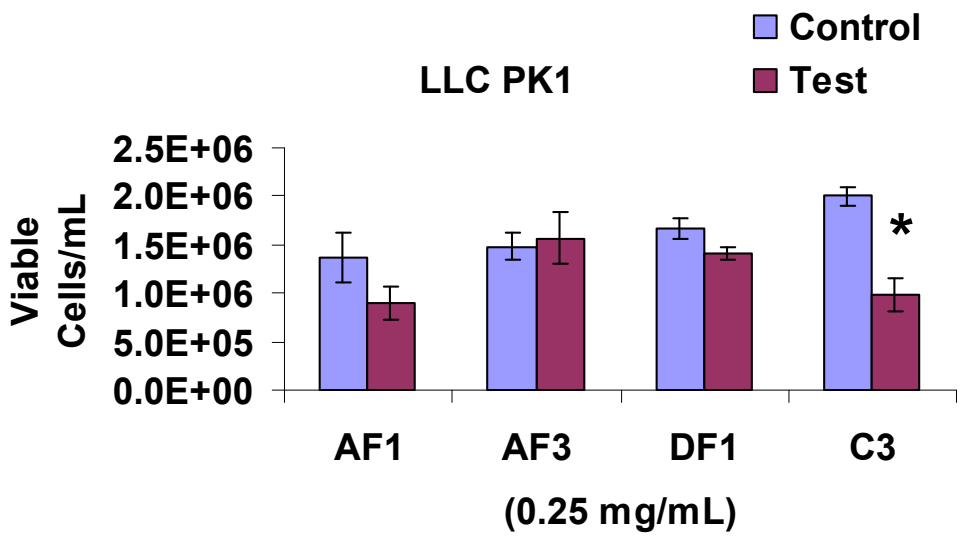

B

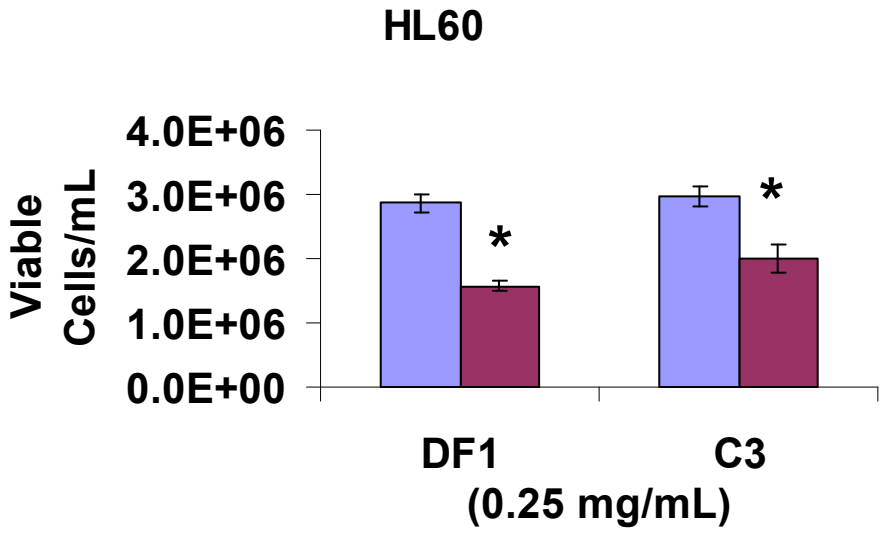

Figure 15. Trypan blue dye-exclusion assay in LLC-PK1 and HL60 cells. LLC-PK1 (**A**) and HL-60 (**B)** cells were treated for 24 hours with 0.25 mg/mL of test samples. Cytotoxicity was determined by the trypan blue dye-exclusion assay, as described in methods**.** The data points are the mean ± the standard error, with *N*=3.

Cell Cycle Effects of DF1 in HL60 Cells

Design and Methods

The purpose of this study was determine if DF1 perturbs cell cycle progression in human leukemia (HL60) cells.

Flow cytometry analysis of the cell cycle in HL60 cells was conducted using propidium iodide nucleic acid staining**.** Briefly, DF1 was diluted to the 0.25 mg/mL test concentration in cell culture media. HL60 cells were plated in 35mm, 6-well format. Cells were preincubated for 24 hours prior to treatment. Cells were treated for 24 hours with 0.25 mg/mL of DF1 in the dark. Following the treatment period, cells were washed with PBS, fixed with ice cold ethanol, and stained with 3 μM propidium iodide for 15 minutes at room temperature. Following staining, cells were analyzed by flow cytometry (ex. 488 nm and em. 617).

Results

Treatment of the HL60 cells with 0.25 mg/mL DF1, resulted in an increase in dead/apoptotic cells (11±1.5% vs. 35±1.9%) and a decrease in G1 (45±0.2% vs. 25±0.8%) and G2/M (19±0.9 vs. 14±0.4) phase cells (Figure 16).

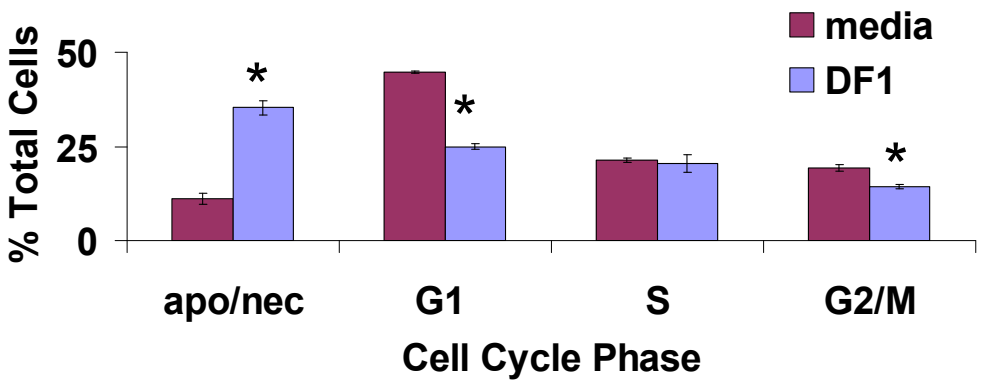

Figure 16. The effect of DF1 on the cell cycle of HL60 cells. HL60 cells were treated for 24 hours with 0.25 mg/mL of DF1. Cell cycle was determined by propidium iodide nucleic acid staining and flow cytometry. Data represents the mean ± the standard error, *N*=3, **P*≤0.05.

Analysis and Conclusions

DF1 appears to primarily target HL60 cells in the G1 phase of the cell cycle.

LC-PK1 and Sprague-Dawley Primary Hepatocyte Reactive Oxygen Species Assay (GTA-7)

Design and Methods

The objective of this study was to determine if AF1, AF3, DF1, or C3 influence reactive oxygen species (ROS) generation in porcine renal proximal tubule (LLC-PK1) and human hepatocarcinoma cells (Hep G2) cell lines.

Reactive oxygen species were measured as described in the Hepatocyte Primary ROS Assay (GTA-7). Briefly, test materials were solubilized via sonication and diluted to the 0.004-1 mg/mL test concentrations in cell culture media. LLC-PK1 cells and Sprague Dawley primary hepatocytes were plated in 96-well, microtiter plate format. Cells were preincubated for 24 hours prior to initial staining, reaching an approximate confluence of 80%. Cells were then incubated in the dark for 30 minutes at 37˚C with 40 μM DCFH, the redox active dye. The wells were then washed with media, and treated with test samples in the dark. Microtiter plate fluorescence was measured at multiple times from 0-4 hours on a spectrophotometer at excitation 485 nm and emission 530 nm.

Results

AF3 was found to fluoresce at the assay wavelengths, and due to this interference was not included in the ROS assay. Treatment of LLC-PK1 cells with AF1 and C3 resulted in a supralinear dose-responsive increase in ROS generation (Figure 17A and C). Treatment of LLC-PK1 cells with DF1, however, resulted in a dose-responsive decrease in ROS generation (Figure 17B).

Treatment of SD primary hepatocytes with AF1 and C3 resulted in a dose responsive increase in ROS generation (Figure18A and C). Treatment SD primary hepatocytes with DF1, however, resulted in a dose responsive decrease in ROS generation.

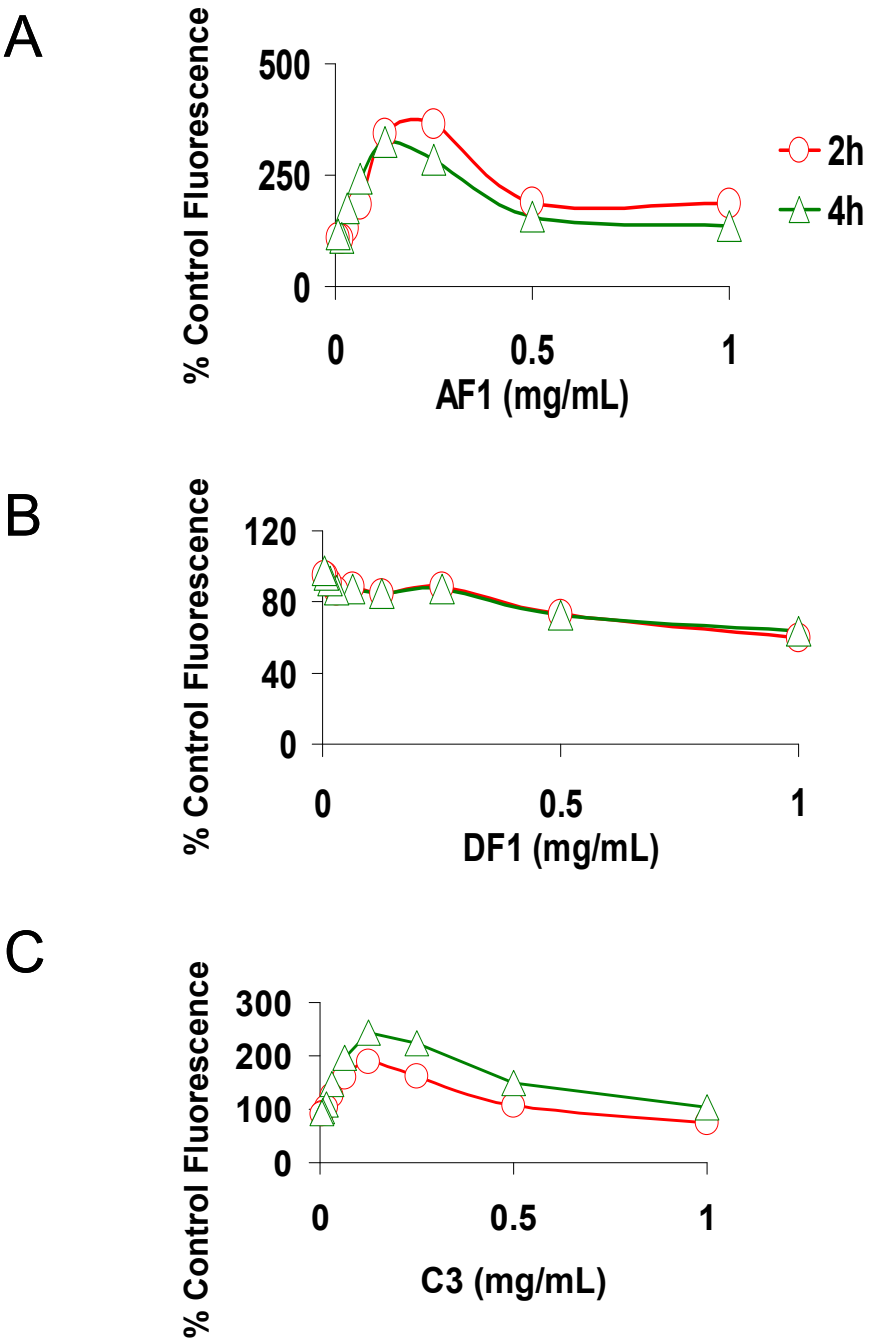

Figure 17. ROS Assay in LLC-PK1 cells. LLC-PK1 cells were treated for 2 and 4 hours with 0.004-1 mg/mL of AF1 (A) DF1 (**B**), or C3 (**C**). ROS was determined as described in described in the Hepatocyte Primary ROS Assay (GTA-7)**,** except that LLC-PK1 cells were used instead of Hep G2 cells**.** Data represents the mean ± the standard error, *N*=3.

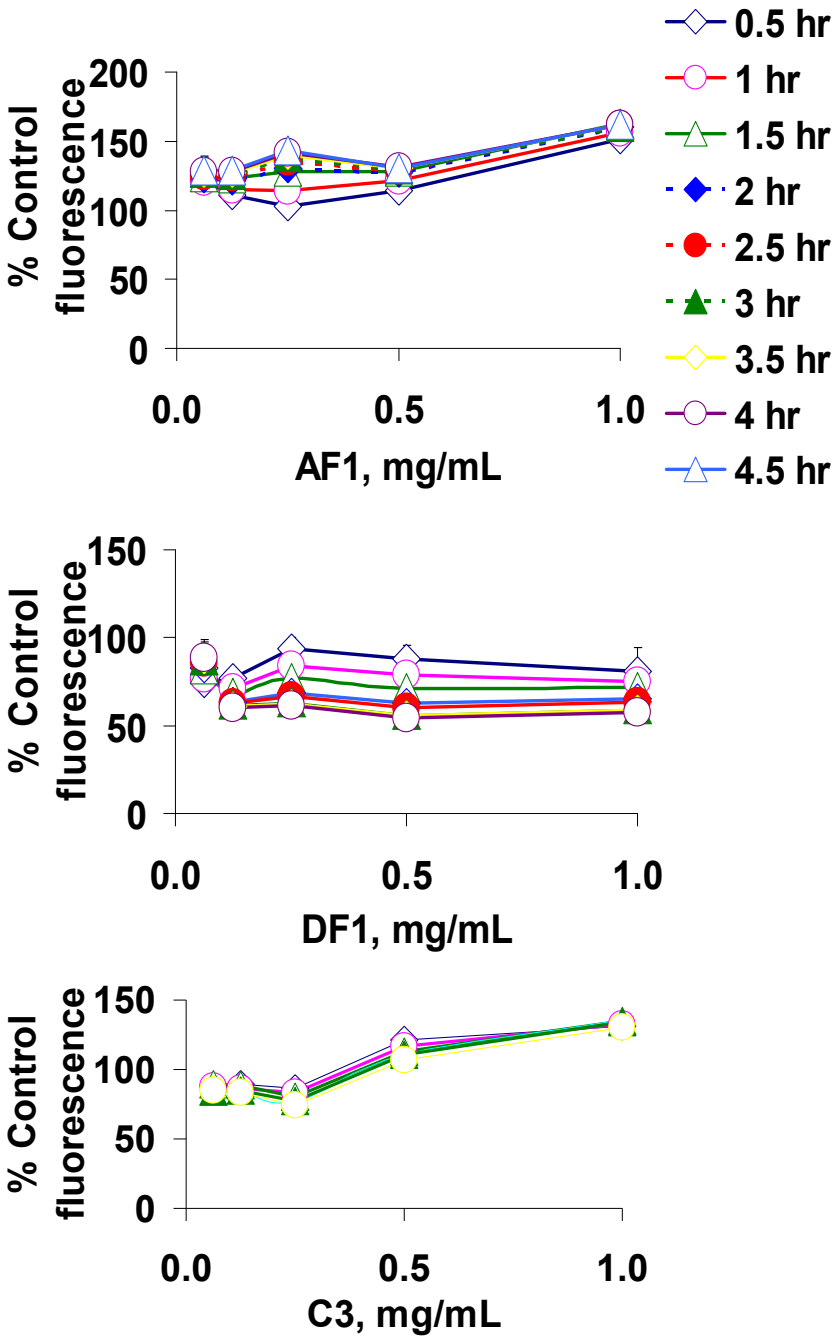

Figure 18. ROS Assay in SD Primary Hepatocytes. SD primary hepatocytes were treated for 0-4 hours with 0.004-1 mg/mL of AF1 (A), DF1 (B), or C3 (C). ROS were measured as described in the Hepatocyte Primary ROS Assay (GTA-7)**.** Data represents the mean ± the standard error with *N*=3.

Analysis and Conclusions

AF1 and C3 were prooxidant, while DF1 was antioxidant in LLC-PK1 cells and SD primary hepatocytes, under these assay conditions. The redox capacity of AF3 could not be determined by the ROS assay method, due to assay interference.

In Vitro Chemoprotection Studies

Section Summary

Cisplatin (CP) is an antineoplastic agent used in the treatment of a variety of solid tumors (Go and Adjei, 1999). The most common dose-limiting toxicity encountered during CP therapy is nephrotoxicity, characterized by tubular necrosis and renal failure (Loehrer and Einhorn, 1984). Oxidative stress has been implicated in CP nephrotoxicity, and studies have shown that antioxidants are effective in preventing toxicity in animal models (Atessahin *et al.*, 2005; Francescato *et al.*, 2004; Nishikawa *et al.*, 2001). Water-soluble fullerenes, which possess exceptional antioxidant properties (Ali *et al,* 2004), are currently undergoing investigation as chemoprotective agents against a variety of oxidative stress-mediated conditions (Lin *et al*, 1999; Lin *et al.*, 2002). The present study examined the potential of the dendritic fullerene derivatives, DF1 and DF1-mini, to prevent CP cytotoxicity in porcine proximal tubule cells. The cotreatment of LLC-PK1 cells with 0.5 mg/mL (180 microM) generation 2 (DF1) or 0.125 mg/mL (90 microM) generation 1 (DF1-mini) dendritic fullerenes resulted in partial protection against 24 hour incubation with 50 microM CP, as determined by cell morphology (Figures 19 and 21). Caspase 3 induction, a measure of apoptosis initiation, was also suppressed >50% by either DF1-mini or DF1 cotreatment (Figures 20 and 23). Pretreatment with DF1 5 hours prior to 4 hour incubation with CP, afforded partial protection against both caspase 3 induction and morphological changes observed at 24 hours (Figures 20 and 21). The fullerene component of DF1 was likely responsible for the observed protection, as the dendritic branches of the derivatized fullerenes independently had no effect (Figure 26). Lipid peroxidation, a marker of oxidative stress, was diminished >25% by DF1 cotreatment at 6 and 24 hours post CP treatment (Figure 27). The mechanism of the observed DF1 and DF1-mini chemoprotection in LLC-PK1 cells is likely amelioration of CP-induced oxidative stress. Future studies will determine if DF1 or DF1-mini also protects against cisplatin nephrotoxicity *in vivo*, while maintaining cisplatin therapeutic properties.

Effect of DF1 Cotreatment on Cisplatin-Induced Apoptosis in LLC-PK1 (GTA-5)

Design and Methods

The objective of this study was to determine the effect of DF1 cotreatment on the induction of apoptosis by cisplatin in porcine renal proximal tubule (LLC-PK1) cells.

In this study, caspase 3 activation was used as a measure of apoptosis. Caspase 3 activity was measured as described in the LLC-PK1 Kidney Apoptosis Assay (GTA-5). Briefly, test materials were diluted to the 0.5 mg/mL test concentration in cell culture media, with or without 50 μM cisplatin. LLC-PK1 cells were plated in 35 mM, 6-well plate format. Cells were preincubated for 24 hours prior to addition of test sample, reaching an approximate confluence of 80%. Cells were treated with test samples in the dark for 24 hours. Following the 24 hour treatment period, the cells were imaged under a light microscope and prepared for caspase 3 activity measurement according to the protocol. Caspase 3 activity was measured using a microtiter plate spectrophotometer at excitation 415 nm and emission 505 nm.

Results

Cotreatment of the LLC-PK1 cells with DF1 afforded partial protection against cisplatin-induced changes in adherent cell density and cell morphology (Figure 19), and reduced caspase 3 activation by 50% (Figure 20).

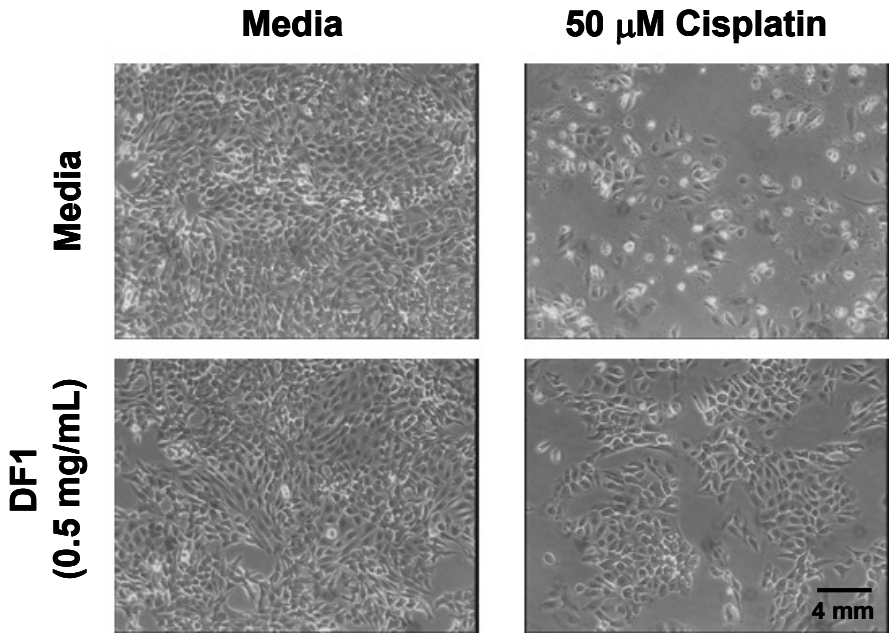

Figure 19. The effect of DF1 cotreatment on 24 hour cisplatin-induced morphological changes. Photomicrographs show representative phase contrast images (x225) of cells treated for 24 hours with 50 μM cisplatin with or without 0.5 mg/mL DF1, or control media.

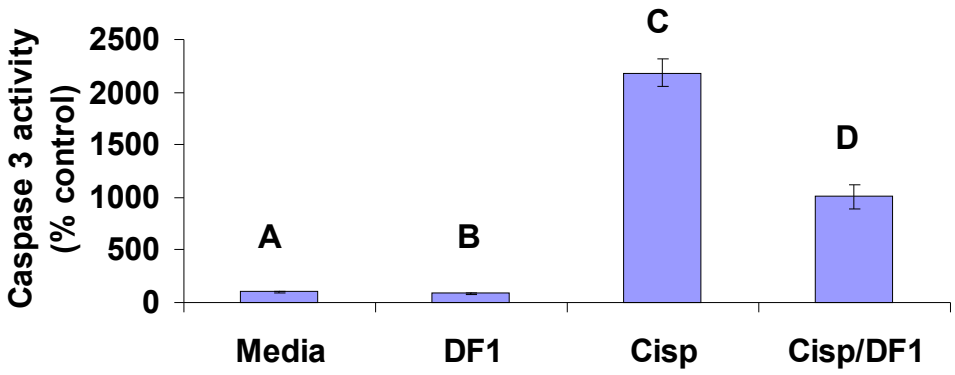

Figure 20. The effect of DF1 cotreatment on 24 hour cisplatin-induced caspase 3 activity. Cells were treated for 24 hours with 50 μM cisplatin (Cisp) with or without 0.5 mg/mL DF1, or control media. Data are presented as % control caspase 3 activity, normalized to total cellular protein. Bars correspond to the mean ± the standard error of six individual samples. Bars with different letters are significantly different from one another ($P \leq 0.05$), as determined by an ANOVA statistical analysis.

Analysis and Conclusions

DF1 cotreatment ameliorated cisplatin-induced morphological changes, and diminished cisplatin-associated casapse 3 activation, a measure of apoptosis. Therefore, DF1 was chemoprotective, under these *in vitro* conditions

Effect of DF1 Pretreatment on Cisplatin-Induced Apoptosis in LLC-PK1 (GTA-5)

Design and Methods

The objective of this study was to determine the effect of DF1 pretreatment on cisplatin-induced apoptosis in porcine renal proximal tubule (LLC-PK1) cells.

In this study, caspase 3 activation was used as a measure of apoptosis. Caspase 3 activity was measured as described in the LLC-PK1 Kidney Apoptosis Assay (GTA-5). Briefly, test materials were diluted to the 0.5 mg/mL test concentration in cell culture media. LLC-PK1 cells were plated in 35 mM, 6-well plate format. Cells were preincubated for 24 hours prior to test sample addition, reaching an approximate confluence of 80%. Cells were treated with test sample in the dark for 5 hours prior to 4 hour incubation with 50 μM cisplatin or control media. At 24 hours post cisplatin treatment, the cells were imaged under a light microscope and prepared for caspase 3 activity measurement according to the protocol. Caspase 3 acivity was measured using a microtiter plate spectrophotometer at excitation 415 nm and emission 505 nm.

Results

Pretreatment of the LLC-PK1 cells with DF1 afforded partial protection against cisplatin-induced changes in adherent cell density and cell morphology (Figure 21), and reduced caspase 3 activation by 25% (Figure 22).

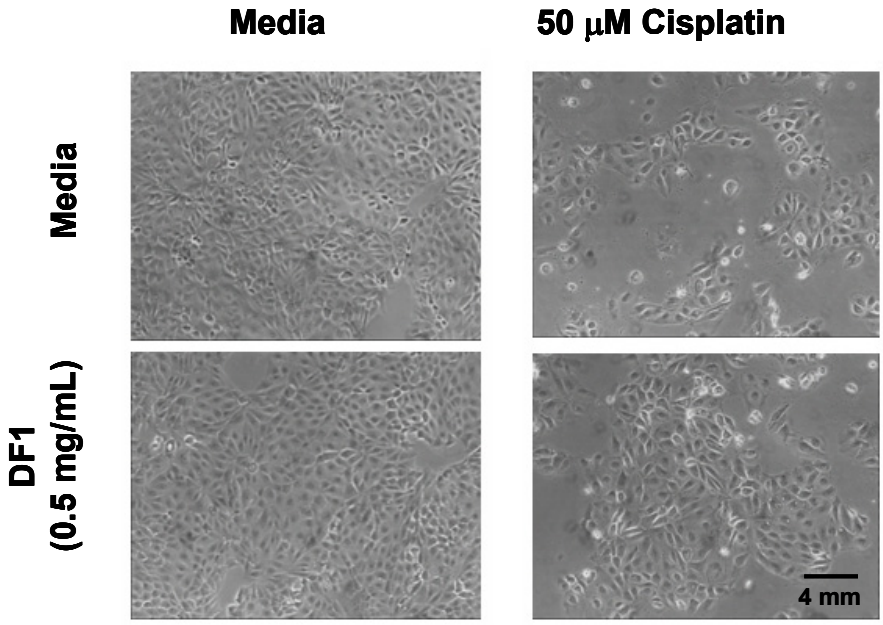

Figure 21. The effect of DF1 pretreatment on 4 hour cisplatin-induced morphological changes. Photomicrographs show representative phase contrast images (x225) of cells treated for 4 hours with 50 μM cisplatin, with or without 5 hours pretreatment with 0.5 mg/mL DF1, or control media.

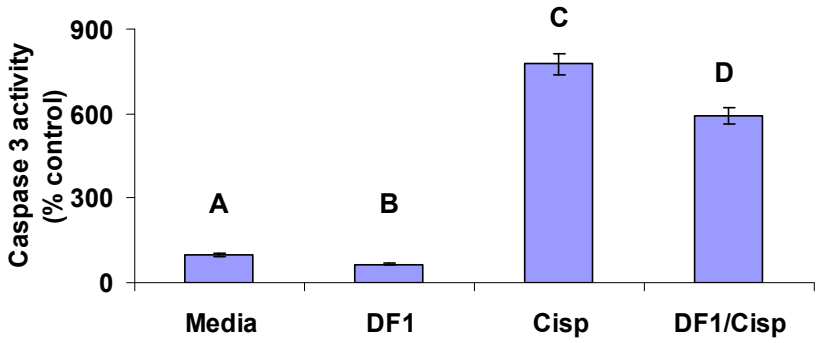

Figure 22. The effect of DF1 pretreatment on 4 hour cisplatin-induced caspase 3 activity. Cells were treated for 4 hours with 50 μM cisplatin (Cisp) with 5 hour pretreatment with 0.5 mg/mL DF1 or control media. Data are presented as % control caspase 3 activity normalized to total cellular protein. Bars correspond to the mean ± the standard error of six individual samples. Bars with different letters are significantly different from one another ($P \leq 0.05$), as determined by an ANOVA statistical analysis.

Analysis and Conclusions

DF1 pretreatment ameliorated cisplatin-induced morphological changes, and diminished cisplatin-associated caspase 3 activation, a measure of apoptosis. Therefore, DF1 was chemoprotective, under these *in vitro* conditions.

Effect of DF1-mini Cotreatment on Cisplatin-Induced Apoptosis in LLC-PK1 (GTA-5)

Design and Methods

The objective of this study was to determine the effect of DF1-mini cotreatment on cisplatin-induced apoptosis in porcine renal proximal tubule (LLC-PK1) cells. DF1-mini is a single generation of dendrimer derivative of DF1.

In this study, caspase 3 activation was used as a measure of apoptosis. Caspase 3 activity was measured as described in the LLC-PK1 Kidney Apoptosis Assay (GTA-5). Briefly, test materials were solubilized via sonication and diluted to the 0.125 mg/mL test concentration in cell culture media, with or without 50 μM cisplatin. LLC-PK1 cells were plated in 35 mM, 6-well plate format. Cells were preincubated for 24 hours prior to addition of test sample, reaching an approximate confluence of 80%. Cells were treated with test samples in the dark for 24 hours. Following the 24 hour treatment period, the cells were imaged under a light microscope and prepared for caspase 3 activity measurement according to the protocol. Caspase 3 acivity was measured using a microtiter plate spectrophotometer at excitation 415 nm and emission 505 nm.

Results

Cotreatment of the LLC-PK1 cells with DF1-mini afforded partial protection against cisplatin-induced changes in adherent cell density and cell morphology (Figure 23), and reduced caspase 3 activation by 65% (Figure 24).

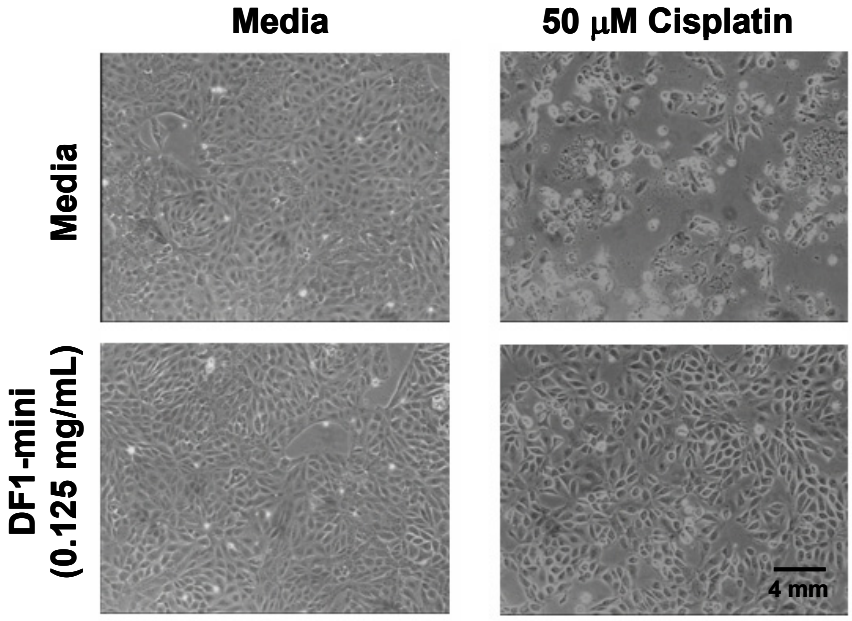

Figure 23. The effect of DF1-mini cotreatment on cisplatin-induced morphological changes. Photomicrographs show representative phase contrast images (x225) of cells treated for 24 hours with 50 μM cisplatin, with or without 0.125 mg/mL DF1-mini, or control media.

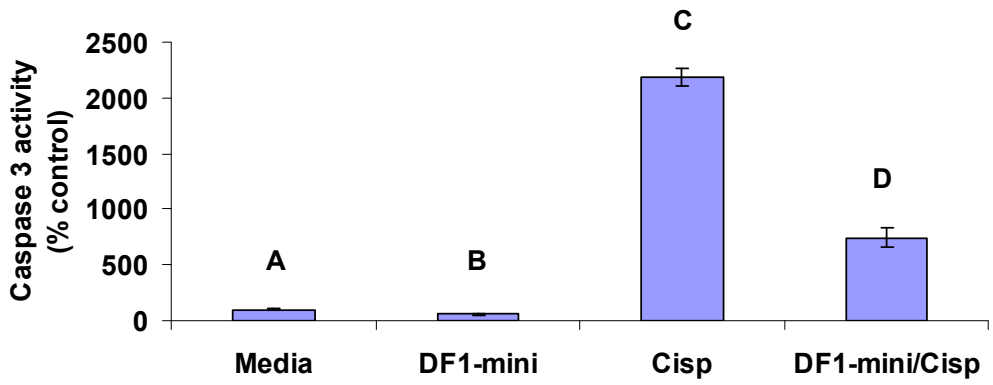

Figure 24. The effect of DF1-mini cotreatment on cisplatin-induced caspase 3 activity. Cells were treated for 24 hours with 50 μM cisplatin (Cisp), with or without 0.125 mg/mL DF1-mini, or control media. Data are presented as % control caspase 3 activity, normalized to total cellular protein. Bars correspond to the mean ± the standard error of six individual samples. Bars with different letters are significantly different from one another ($P \leq 0.05$), as determined by an ANOVA statistical analysis.

Analysis and Conclusions

DF1-mini cotreatment ameliorated cisplatin-induced morphological changes, and diminished cisplatin-associated casapse 3 activation, a measure of apoptosis. Therefore, DF1-mini was chemoprotective, under these *in vitro* conditions.

Effect of AP12 and AP36 Cotreatment on Cisplatin-Induced Apoptosis in LLC-PK1 (GTA-5)

Design and Methods

The objective of this study was to determine if the dendritic branches of DF1 or DF1-mini were involved in the mechanism of cisplatin chemoprotection. For example, the carboxylic acid terminated dendritic arms could conceivablly chelate cisplatin, thereby limiting access of cisplatin to the cell. In order to address this possibility, porcine renal proximal tubule (LLC-PK1) cells were cotreated with cisplatin and the control dendrimers, AP12 or AP36 (structure, Figure 25) without C60 component. AP12 corresponds to the dendritic architecture of DF1-mini and contains 12 terminal carboxylic acid groups, AP36 corresponds to the dendritic arms of DF1 with 36 terminal carboxylic acid groups.

In this study, caspase 3 activation was used as a measure of apoptosis. Caspase 3 activity was measured as described in the LLC-PK1 Kidney Apoptosis Assay (GTA-5). Briefly, test materials diluted to the 0.125 mg/mL test concentration in cell culture media, with or without 50 μM cisplatin. LLC-PK1 cells were plated in 35 mM, 6-well plate format. Cells were preincubated for 24h prior to addition of test sample, reaching an approximate confluence of 80%. Cells were treated with test samples for 24 hours in the dark. Following the 24 hour treatment period, the cells were imaged under a light microscope and prepared for caspase 3 activity measurement according to the protocol. Caspase 3 activity was measured using a microtiter plate spectrophotometer at excitation 415 nm and emission 505 nm.

Results

Cotreatment of the LLC-PK1 cells with AP12 or AP36 afforded no protection against cisplatin-induced capase 3 activation (Figure 26).

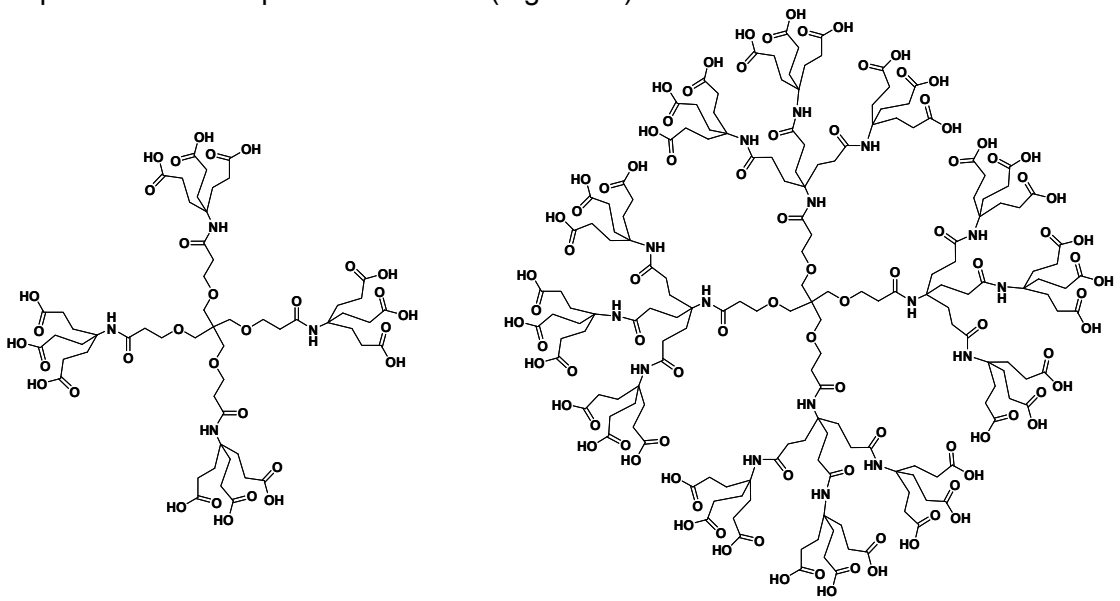

AP12 AP36

Figure 25. The chemical structures of AP12 and AP36.

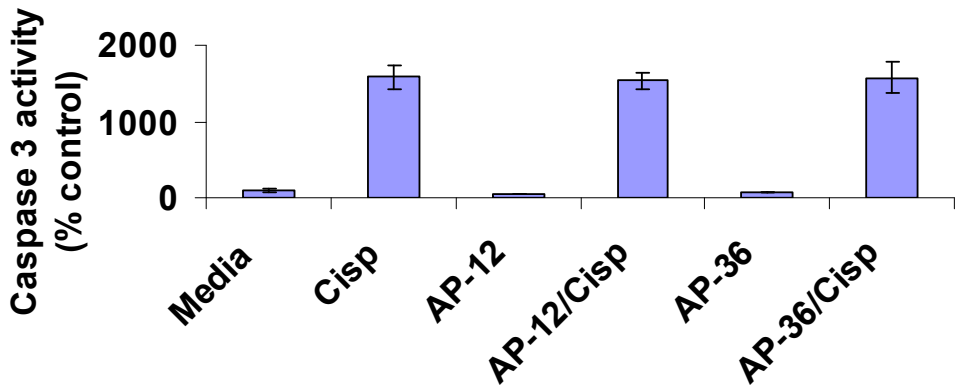

Figure 26. The effect of AP12 or AP36 cotreatment on cisplatin-induced caspase 3 activity. Cells were treated for 24 hours with 50 μM cisplatin (Cisp) with or without 0.34 mg/mL AP12, AP36, or control media. Data are presented as % control caspase 3 activity normalized to total cellular protein. Bars correspond to the mean ± the standard error of six individual samples.

Analysis and Conclusions

Since AP12 and AP36 had no effect on cisplatin-induced apoptosis in the LLC-PK1 cells, this suggest that the fullerene component and not the carboxylic acid terminated dendritic arms of DF1 and DF1-mini are involved in the mechanism underlying the observed chemoprotection

Effect of DF1 Cotreatment on Cisplatin-Induced Lipid Peroxidation (GTA-4)

Design and Methods

The objective of this study was to determine if DF1 cotreatment could diminish cisplatin-induced lipid peroxidation. Cisplatin-induced cytotoxicity is associated with lipid peroxidation both *in vivo* and *in vitro* (Sugihara *et al.*, 1987a; Sugihara *et al.*, 1987b). If the mechanism of DF1 chemoprotection in LLC-PK1 cells involves amelioration of cisplatin-induced oxidative stress, then DF1 should suppress lipid peroxidation.

In this study, lipid peroxides in the LLC-PK1 cells were measured as described in the Hep G2 Hepatocyte Lipid Peroxidation Assay (GTA-4). Briefly, test materials were solubilized via sonication and diluted to the 0.125 mg/mL test concentration in cell culture media, with or without 50 μM cisplatin. LLC-PK1 cells were plated in 35 mM, 6-well plate format. Cells were preincubated for 24 hours prior to addition of test sample, reaching an approximate confluence of 80%. Cells were treated with test samples in the dark for 6 and 24 hours. Following the treatment periods, the cells were prepared for TBARS measurement according to the GTA-4 protocol. TBARS were measured using a microtiter plate spectrophotometer at excitation 415 nm and emission 505 nm.

Results

Cotreatment of the LLC-PK1 cells with DF1, suppressed the cisplatin-induced lipid peroxidation 65% and 74%, at the 6 and 24 hour time points, respectively (Figure 27).

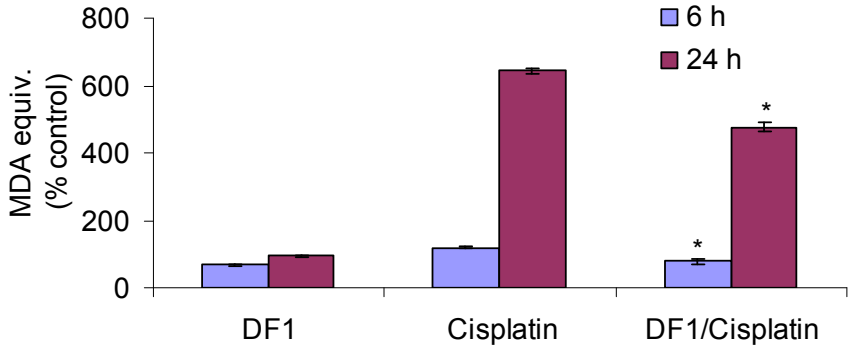

Figure 27. The effect of DF1 pretreatment on cisplatin-induced lipid peroxidation. Cells were treated for 6 and 24 hours with 50 μM cisplatin with or without 0.5 mg/mL DF1. Data are presented as % control MDA equivalents in the incubation media, normalized to total cellular protein. Bars correspond to the mean ± the standard error of three individual samples. Bars marked with asterisks have $P<0.05$ *versus* cisplatin treatment, by Student's *t* –test.

Analysis and Conclusions

Since DF1 decreased cisplatin-induced lipid peroxidation in the LLC-PK1 cells, this suggests that the mechanism underlying the observed chemoprotection by DF1 may involve amelioration of oxidative stress

In Vitro Immunological Characterization

Section Summary

This is a study of the effects of the C-Sixty, Inc. fullerene derivatives on the integrity of red blood cells, platelet aggregation, and formation of granulocyte-macrophage colonies (CFU-GM). The analyses were performed using three NCL imunotoxicity assays: ITA-1 (assay for hemolysis), ITA-2 (platelet aggregation) and ITA-3 (CFU-GM assay). The procedures for these NCL assays are detailed in the August 2006 NCL *In Vitro* Protocols. AF1 and AF3 demonstrated hemolytic properties on human erythrocytes, while C3 and DF1 did not affect the integrity of erythrocytes. None of the tested fullerene derivatives induced platelet aggregation, however C3 and DF1 suppressed aggregation of platelets induced by collagen. None of the tested fullerene derivatives were myelosuppressive or capable of preventing cisplatin-induced toxicity to bone marrow haematopoietic stem cells.

Nanoparticle Hemolytic Properties (ITA-1)

Design and Methods

The objective of this study was to evaluate four fullerene derivatives: AF1, AF3, DF1, and C3 in terms of their effects on the integrity of red blood cells. Stock solutions with theoretical concentration of 1mg/mL were used for each C60 derivative. The resulting final nanoparticle concentration was 125 μg/mL . NCL protocol ITA-1 was followed. Poly-L-lysine (PLL) and polyethyleneglycol (PEG) were used as positive and negative controls, respectively.

Results

At tested concentrations, AF1 resulted in >85% hemolysis. AF3 was also hemolytic (% hemolysis >10), while C3 and DF1 did not disturb the integrity of red blood cells (Figure 28).

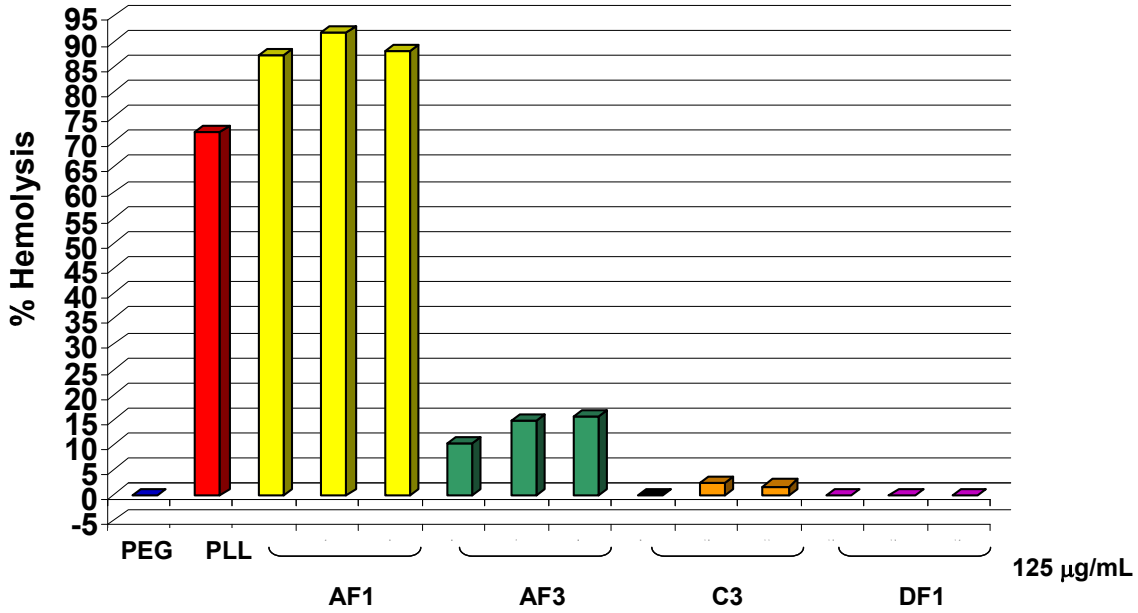

Figure 28. Analysis of nanoparticle hemolytic properties (ITA-1). 125 μg/mL samples of AF1, AF3, C3 and DF1 were tested for effects on the integrity of red blood cells. Three independent samples were prepared for each nanoparticle sample and analyzed in duplicate (%CV<20). Each bar represents the mean of duplicate results. Poly-L-lysine (PLL) and polyethyleneglycol (PEG) were used as positive and negative controls, respectively. AF1 and AF3 were hemolytic, while C3 and DF1 did not disturb the integrity of red blood cells.

Analysis and conclusions

AF1 and AF3 are capable of inducing damage to red blood cells *in vitro*. C3 and DF1 do not have hemolytic properties when tested *in vitro*.

Nanoparticle Ability to Induce Platelet Aggregation (ITA-2)

Design and Methods

The objective of the study was to evaluate four C60 derivatives: AF1, AF3, DF1, and C3, in terms of their effects on human platelet aggregation *in vitro*. Stock solutions with concentrations of 1 mg/mL were used for each C60 derivative. The final nanoparticle concentrations after dilution according to the ITA-2 protocol were 200 μg/mL. Three independent samples were prepared for each nanoparticle formulation and analyzed in duplicate (%CV<20%). NCL protocol ITA-2 was followed. Collagen was used as positive control.

Results

At tested concentrations, none of the C60 derivatives induced platelet aggregation (all tested fullerene derivatives showed % aggregation <10). When platelet aggregation was induced by collagen, AF1 did not interfere with this process. AF3 resulted in approximately a 30% decrease in collagen-induced platelet aggregation. C3 and DF1 prevented platelet aggregation caused by collagen (Figure 29).

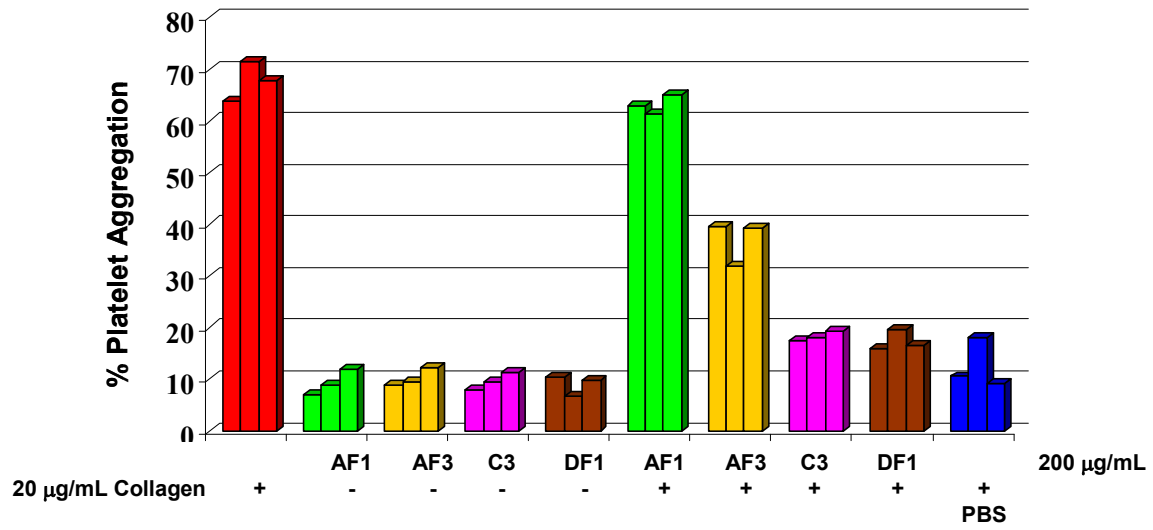

Figure 29. Analysis of nanoparticle ability to induce platelet aggregation (ITA-2). AF1, AF3, C3 and DF1 at a final concentration of 200 μg/mL were used to evaluate potential particle effects on the cellular component of the blood coagulation cascade. Collagen was used as positive control. The effects of the fullerene derivatives on collagen induced aggregation were studied by combining collagen with the nanoparticle treatments. Three independent samples were prepared for each nanoparticle formulation and analyzed in duplicate (%CV<20%). Bars represent the mean of duplicate results. None of the tested formulations induced platelet aggregation. AF1 did not interfere with collagen-induced aggregation, AF3 resulted in approximately a 30% decrease in collagen-induced platelet aggregation, and DF1 and C3 prevented aggregation of platelets in response to collagen.

Analysis and Conclusions

None of the C60 derivatives induced platelet aggregation. AF3 resulted in a decrease in collagen-induced platelet aggregation. C3 and DF1 prevented collagen-induced platelet aggregation.

Nanoparticle Toxicity to Bone Marrow Cells (ITA-3)

Design and Methods

The objective of this study was to evaluate the four C60 derivatives: AF1, AF3, DF1, and C3, in terms of their myelosuppressive effects. Since previous toxicology studies indicated DF1 was chemoprotective in kidney cell models, we also examined protection from cisplatin-induced myelosuppression. Stock solutions with theoretical concentrations of 1 mg/mL were used for each C60 derivative. The final nanoparticle concentrations of all formulations were 50 μg/mL. NCL protocol ITA-2 was followed. Hematopoietic stem cells were isolated from the bone marrow of 8-12 week old C57BL/6 mice. The cells were cultured for 12 days in MethoCult media supplemented with cytokines in the presence of PBS (a negative control), cisplatin (a positive control), and the C60 derivatives (to test for myelosuppressive properties) or a combination of cisplatin and the C60 derivatives (to test for chemoprotective properties). Two independent samples of each formulation were prepared and analyzed in duplicate.

Results

None of C60 derivatives was toxic to hematopoietic stem cells as indicated by undisturbed granulocyte and macrophage colonies formation (Figure 30). At tested concentrations, none of the C60 derivatives was capable of reducing or preventing cisplatin's toxicity to granulocyte and macrophages precursors (Figure 30).

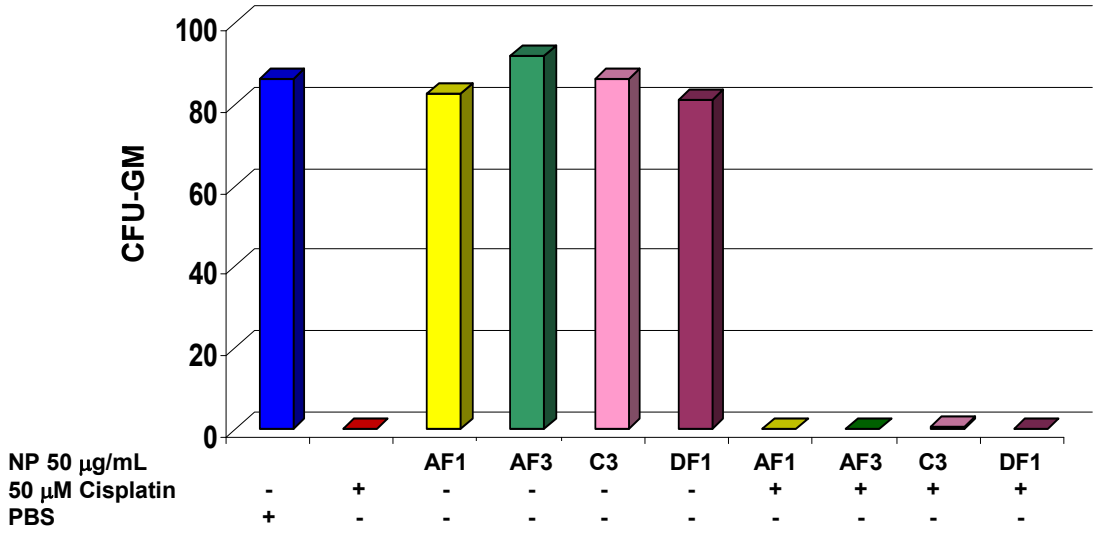

Figure 30. Analysis of nanoparticle toxicity to bone marrow cells (ITA-3). Two independent samples were prepared and analyzed in duplicate. Each bar represents the mean of duplicate responses (%CV <25). Results indicate that none of the tested particles was myelosuppressive or capable of protecting granulocyte-macrophage precursors from cisplatin cytotoxicity. NP stands for nanoparticle. All nanoparticle samples had concentrations of 50 μg/mL

Analysis and Conclusions

None of C60 derivatives was toxic to hematopoietic stem cells or protective from cisplatin's toxicity to granulocyte and macrophages precursors

Contributors

Nanotechnology Characterization Laboratory Staff:

Scott E. McNeil, Ph.D., Director
Anil K. Patri, Ph.D., Senior Scientist
Stephen T. Stern, Ph.D., Scientist
Marina Dobrovolskaia, Ph.D., Scientist
Jiwen Zheng, Ph.D., Scientist
Jeffrey Clogston, Ph.D., Scientist
Banu S. Zolnik, Ph.D., Postdoctoral Fellow
Chris McLeland, Senior Research Associate
Timothy M. Potter, Research Associate
Barry W. Neun, Research Assistant
Sarah Skoczen, M.S., Research Assistant

Jack Simpson, Ph.D., Protein Chemistry Laboratory
King Chan, M.S., Laboratory of Proteomics and Analytical Technologies

Abbreviations

2D PAGE Two-Dimensional Polyacrylamide gel Electrophoresis
51Cr 51 Chromium
ABN Abnormal Plasma Standard
AFFF Asymmetrical Field Force Fractionation
APTT Activated Partial Thromboplastin Time
ATCC American Type Culture Collection
AUC Area Under the Curve
CBA Cytometric Bead Array
CE Capillary Electrophoresis
CFU-GM Colony Forming Units-Granulocyte Macrophage
Cisp Cisplatin
CP Cisplatin
CV Coefficient of Variation
CVF Cobra Venom Factor
DHB 2,5-dihydroxybenzoic acidDI
(H2O) Deionized H2O
DLS Dynamic Light Scattering
E:T ratio Effector: Target Ratio
ELISA Enzyme-Linked Immunosorbent Assay
FBS Fetal Bovine Serum
FDA Food and Drug Administration
HEP-G2 Human Hepatocarcinoma Cells
HPLC High Performance Liquid Chromatography
IL InterleukinK562 Human Erythroleukemia Cell Line
kDa Kilodalton
kV KiloVolt
LAL Limulus Activation Lysate
LDH Lactate Dehydrogenase
LEI Laboratory of Experimental Immunology
LLC-PK1 Porcine Renal Proximal Tubule Cells
LPS Lipopolysaccharide
MALDI-TOF Matrix Assisted Laser Desorption/Ionization – Time of Flight
mg Milligram
mL Milliliter
mm Millimeter
MS Mass Spectroscopy
MTT 3-(4,5-dimethyl-2-thiazolyl)-2,5-diphenyl-2H-tetrazolium bromide
N Normal plasma standard
NCL Nanotechnology Characterization Laboratory
NIST National Institute of Standards and Technology
NO Nitrous Oxide
PBMC Peripheral Blood Mononuclear Cells
PBS Phosphate Buffered Saline
PHA-M Phytohemaglutinin-M
psi Pounds per Square Inch
PT Prothrombin Time
RDG Rayleigh-Debye- Gans
RAW 264.7 Mouse Leukemic Macrophage Monocyte Cell Line

ROS Reactive Oxygen Species
RT-CES Real Time- Cell Electronic Sensing
SAIC Science Applications International Corporation
SPGR Spoiled Gradient Echo Sequences
Unt Untreated
UV-Vis Ultra Violet- Visible
v/v volume/volume

References

Ali, S.S., Hardt, J.I., Quick, K.L., Kim-Han, J.S., Erlanger, B.F., Huang, T.T., Epstein, C.J., and Dugan, L.L. (2004). A biologically effective fullerene (C60) derivative with superoxide mimetic properties. Free Radic Biol Med 37, 1191-202.

Atessahin, A., Yilmaz, S., Karahan, I, Ceribasi, A.O., and Karaoglu, A. (2005). Effects of lycopene against cisplatin-induced nephrotoxicity and oxidative stress in rats. Toxicology 212, 116-23.

De Lorenzo AJ. 1970. The olfactory neuron and the blood-brain barrier. In: Taste and Smell in Vertebrates (Wolstenholme G, Knight J, eds). London:Churchill, 151–176.

Duncan, R. (1999). Polymer conjugates for tumor targeting and intracytoplasmic delivery. The EPR effect as a common gateway Pharm. Sci. Technol. Today 2, 441-49.

Francescato, H.D., Coimbra, T.M., Costra, R.S., and Biachi Mde, L. (2004). Protective effect of quercetin on the evolution of cisplatin-induced acute tubular necrosis. Kidney Blood Press Res27, 148-58

Foley S, Crowley C, Smaihi M, Bonfils C, Erlanger BF, Seta P, et al. Cellular localisation of a water-soluble fullerene derivative. Biochem Biophys Res Commun. 2002;294:116–119.

Gharbi, N., Burghardt, S., Brettreich, M., Herrenknecht, C., Tamisier-Karolak, S., Bensasson, R., Szwarc, H., Hirsch, A., Wilson, S.R., and Moussa, R. (2003) Chromatographic Separation and Identification of a Water-Soluble Dendritic Methano[60]fullerene. Octadecaacid, Anal. Chem. 75, 4217-4222

Go, R.S., and Adjei, A.A. (1999). Review of the comparative pharmacology and clinical activity of cisplatin and carboplatin. J Clin Oncol 17, 409-22.

Lin A.M., Fang S.F., Lin S.Z., Chou C.K., Luh T.Y., Ho L.T. (2002) Local carboxyfullerene protects cortical infarction in rat brain. Neurosci Res. 43, 317-21.

Lin AM, Chyi BY, Wang SD, Yu HH, Kanakamma PP, Luh TY, Chou CK, Ho LT. (1999). Carboxyfullerene prevents iron-induced oxidative stress in rat brain.
J Neurochem 72, 1634-40.

Loehrer, P. J. and Einhorn, L.H. (1984). Drugs five years later. Cisplatin. Ann Intern Med 100, 704-13.

Nishikawa, M., Nagatomi, H., Nishijima, M., Ohira, G., Chang, B.J., Sato, E., and Inoue, M. (2001). Targeting superoxide dismutase to renal proximal tubule cells inhibits nephrotoxicity of cisplatin and increases the survival of cancer bearing mice Cancer Lett 171, 133-8)

Sayes, C.M., Fortner J.D., Guo, W., Lyon, D., Boyd, A.M., Ausman, K.D., Tao, Y.J., Sitharaman, Balaji, Wilson, L.J., Hughes, J.B., West J.L., and Colvin, V.L. (2004) The Differential Cytotoxicity of Water-Soluble Fullerenes. Nano Letters 4, 1881-87.